BIOELECTRICITY
Volume 3, Number 1, 2021

DOI: 10.1089/bioe.2019.0034

Original Research

A Meta-Analysis of Bioelectric Data in Cancer, Embryogenesis, and Regeneration

Pranjal Srivastava,[1] Anna Kane, PhD,[2] Christina Harrison,[2] and Michael Levin, PhD[2]

Abstract

Developmental bioelectricity is the study of the endogenous role of bioelectrical signaling in all cell types. Resting potentials and other aspects of ionic cell physiology are known to be important regulatory parameters in embryogenesis, regeneration, and cancer. However, relevant quantitative measurement and genetic phenotyping data are distributed throughout wide-ranging literature, hampering experimental design and hypothesis generation. Here, we analyze published studies on bioelectrics and transcriptomic and genomic/phenotypic databases to provide a novel synthesis of what is known in three important aspects of bioelectrics research. First, we provide a comprehensive list of channelopathies—ion channel and pump gene mutations—in a range of important model systems with developmental patterning phenotypes, illustrating the breadth of channel types, tissues, and phyla (including man) in which bioelectric signaling is a critical endogenous aspect of embryogenesis. Second, we perform a novel bioinformatic analysis of transcriptomic data during regeneration in diverse taxa that reveals an electrogenic protein to be the one common factor specifically expressed in regeneration blastemas across Kingdoms. Finally, we analyze data on distinct V_{mem} signatures in normal and cancer cells, revealing a specific bioelectrical signature corresponding to some types of malignancies. These analyses shed light on fundamental questions in developmental bioelectricity and suggest new avenues for research in this exciting field.

Keywords: cancer, development, channelopathy, V_{mem}, resting potential, regeneration, ion channel

Introduction

Bioelectrical signaling is an ancient modality by which cells and tissues exchange information necessary for coordinating development, regeneration, and cancer suppression.[1–4] Many details have now been uncovered about the ion channels and pumps that determine cell membrane resting potential (V_{mem}) and about the electrical synapses known as gap junctions that propagate those states across distances *in vivo*.[5] Using a range of model species, modern developmental biology and genetics efforts have identified roles of bioelectrical signaling in cell migration,[6,7] organ morphogenesis,[8–10] regenerative axial polarity,[11] size control,[12] and many other important metazoan phenomena. The implications of these results stretch from basic evolutionary developmental biology[13,14] to many aspects of biomedicine.[15–19]

However, this exciting emerging field has been hampered by the fact that, due to its highly interdisciplinary nature, important data are spread across publications in numerous subfields and have not been analyzed *en masse*. Thus, we undertook a synthesis and meta-analysis of data from published studies to ask several fundamental questions in three deeply related subfields: development, regeneration, and cancer.

How important is bioelectricity in embryogenesis? It is often thought that the roles of ion channels are only apparent from a handful of focused studies,[10,20–22] and that genetics does not offer a convenient entry point to discover novel bioelectric controls. Thus, we analyzed databases of developmental phenotypes across a number of popular model systems to identify a comprehensive list of electrogenic genes that have been implicated in embryonic patterning.

Cancer can be thought of as a breakdown of the normal processes that orchestrate cells into cooperating toward production and maintenance of large-scale anatomical structures during development and adulthood.[23–26] Interestingly, classical[27,28] and recent[29–32] functional data suggest that control of bioelectric signaling can not only induce cancer phenotypes but can also be used to suppress/normalize tumors. Can bioelectric parameters be used to distinguish between normal somatic cells and those that have defected back into a unicellular-like state (transformed cancer cells)? We thus attempted to identify every published study of resting potential

[1]Rye High School, Rye, New York, USA; *Current Affiliation*: College of Chemistry, University of California, Berkeley, Berkeley, California, USA.
[2]Department of Biology, Allen Discovery Center, Tufts University, Medford, Massachusetts, USA.

in cells and analyzed them to derive a physiological signature of the transformed state across different tissue types.

Regeneration is a process by which complex organs and appendages are rebuilt to a specific target morphology from various starting states (injuries).[33] The evolutionary origins of this capability across taxa are poorly understood,[34] and it is unclear what molecular-genetic and biophysical components underlie regeneration of different types of body architectures. Thus, we analyzed transcriptomic datasets comparing regenerating versus intact adult tissues across Kingdoms, asking what types of regeneration-induced gene expression changes they might share. A small number of genes turned out to be a common feature of regeneration in all animals, from flatworms to mammals. Remarkably, analysis taking into account plants revealed only one component that all regenerating blastemas have in common: an ancient electrogenic protein.

Development, regeneration, and cancer have a profound connection. The first two concern the ability of cells to work together to, respectively, build and rebuild complex anatomical structures. The third, cancer, illustrates the effects of individual somatic cells abandoning multicellularity and reverting to a unicellular mode of existence that treats the rest of the body as its environment. In all of these cases, communication and interaction among cell groups are paramount. Evolution discovered very early how to exploit biophysical forces to coordinate information across space and time in living cells and tissues.[35–37] It is now essential, for biomedicine and for evolutionary developmental biology, to understand how the molecular mechanisms of bioelectricity enable cooperative cell function in normal morphogenesis and its disruption during disease.[38,39] Together, the following meta-analyses establish a rigorous starting point for novel work in this field, revealing a range of physiological and genetic targets for future investigation and shedding light on foundational concepts in developmental bioelectricity.

Materials and Methods

Literature search for V_{mem} values in somatic and cancerous cells

Literature search was completed in two distinct phases: first, the keywords ''Vmem,'' ''Electrical Potential,'' ''Electrophysiological properties,'' and ''Membrane Potential'' were used singly and in combination in PubMed searches. Published V_{mem} values and their sources were documented in a database to avoid duplication. After all potential papers that could be found using this method were exhausted, existing meta-analyses such as those found in previous studies[40,41] were mined for any additional papers that contained V_{mem} values. These published studies were then themselves included in our analysis. We decided to only include data from rodent and human cells in our analysis because the vast majority of the papers focused on these models and data from other systems did not provide sufficient power for analysis.

Statistical analysis

Meta-analyses were performed to assess relationships between reported V_{mem} in cancerous and noncancerous tissues. A random-effects meta-analysis was performed to assess the relationship between reported mean V_{mem} in cancerous tissues and their corresponding somatic tissue type. Statistics were only performed on tissues for which there was both somatic and cancerous measurements taken in the same report. Analysis was performed with the rma function from the Metafor (v2.0-0) R package. p-value was considered significant at $p < 0.05$, and tests for heterogeneity were performed in each case.

To assess the relationship between the V_{mem} of a somatic tissue and the difference in V_{mem} between it and the V_{mem} of a corresponding cancerous tissue, a mixed-effect regression model was used. We modeled the change in voltage from somatic tissue to cancerous tissue as a linear function of the mean somatic voltage, and included all studies that provided estimates of both means and variability for both cell types. The rma function from the Metafor (v2.0-0) R package was used for this analysis. A least-squares regression was done as sensitivity analysis that included additional studies where estimates of within-study variation were not provided. All studies were equally weighted in this analysis. The lm function in the stats (v3.5.3) R package was used to estimate the linear regression line. p-value was considered significant at $p < 0.05$, and tests for heterogeneity were performed in each case.

Statistics were performed by the Tufts Biostatistics, Epidemiology, and Research Design Center. R version 3.5.3 (2019-03-1) run through R Studio v1.1.463 (c) 2009–2018, R Studio, Inc. was used to perform the meta-analyses. Raw p-values are reported without adjustment for multiple testing.

Channelopathy identification database and literature search

To identify as many ion channel-associated developmental and morphological phenotypes as possible, we searched species-specific databases that report phenotypes associated with genetic mutations. We primarily focused on phenotype databases to ensure that we had the broadest phenotype report possible, since these databases do not require that the phenotypes induced by genetic mutation be interesting enough to rise to the level of publication. In addition to ion pumps and channels, both of which establish bioelectrical potentials, gap junctions are important because they enable cells to communicate that bioelectric state to each other,[5,42] and because their voltage-based and other gating modalities enable cell collectives to form networks, which process bioelectrical information in complex ways, such as forming feedback loops and even computational circuits.[43,44] Thus, here we broaden the term ''channelopathy'' to include those induced by mutations in ion pumps and gap junctions, not only strictly ion channel proteins, because of the similar, crucial roles of these other two types of proteins in regulating the bioelectric state of cells.

Human channelopathies were identified from long-term, manual curation of publications that assess developmental phenotypes linked to genetic screens or clinically identified syndromes. Mouse channelopathies were identified through keyword searches in the MGI database[45] for terms, including ''channel,'' ''pump,'' ''transporter,'' ''antiporter,'' ''gap junction,'' and ''connexin'' (and manually filtered to include only electrically relevant targets). Each entry was searched for morphogenesis and developmental phenotypes in the ''Mutations, Alleles and Phenotypes'' section, and the phenotype was verified in the reported primary literature. To identify zebrafish channelopathies, the database Zfin[46] was used. Keyword searches for ''Pannexin,'' ''Innexin,'' ''Ion Channel,'' and

''Ion Junction'' were carried out to identify channelopathies, and morphogenesis phenotypes were identified in the ''Disease Ontology'' and ''Gene Ontology'' sections of each entry. Each phenotype identified was verified in the reported primary literature. Flybase[47] was used to identify channelopathies in *Drosophila.* Keyword searches for ''Ion Channel,'' ''Pannexin,'' ''Ion Pump,'' and ''Ion Transporter'' were performed, and each entry was searched for developmental and morphogenesis phenotypes in the ''Phenotype'' section of the entry.

Additional genes mentioned in known papers (previously identified through PubMed searches) on ion channels in *Drosophila* were also included (and referenced accordingly), particularly, Smith et al.[8] which contained a long list of wing-related *Drosophila* channelopathies. Each phenotype was verified in the reported primary literature. Genes identified in the Flybase search were also assessed using the Bristle Screen Online Database,[48] which provided more detailed analyses of morphogenesis defects than Flybase alone. For the *Caenorhabditis elegans*, we created an XML code that searched Wormbase (release WS271) for patterning defects. The code was provided by one of the curators of the database, Christian A. Grove.

The results that gave multiple patterning defects for one gene were condensed into one entry. Identified entries were then individually assessed for ion channel activity and morphogenesis or developmental defects and confirmed in the reported primary literature.

Bioinformatics

Datasets containing lists of up- and downregulated transcripts in regeneration blastemas of axolotl (*Ambystoma mexicanum*, NCBI SRA064951),[49] planarian head and tail fragments (*Schmidtea mediterranea*, NCBI SRP002478),[50] deer antler (*Cervus nippon*, BioProject IDs: PRJNA397466 and PRJNA404007), and plant (*Arabidopsis thaliana,* NCBI GSE19863) were obtained from published supplementary data,[49,50] NCBI SRA,[51] or NCBI GEO.[52] Annotation for the planaria dataset was obtained from eggNOG-mapper.[53,54]

Some of the datasets only provided F-tests for significant results but did not provide information about direction of fold change. Thus, all significantly altered transcripts, both up- and downregulated, were combined and considered as one pool. Genes with false discovery rate (FDR) <0.25 were considered significantly altered. All significantly altered genes in each dataset were then crossreferenced to identify any transcripts that were commonly differentially expressed across model systems.

For gene set enrichment analysis, ''background'' genes were assigned in each model organism based on protein homology to human protein-coding gene sequences obtained from BioMart. Gene Ontology sets were acquired from the MSigDB Collections.[55] Gene sets related to ion channels and cell junctions or learning, memory, and cognition were selected, and Fisher's exact tests were performed to determine enrichment. FDR <0.25 was considered significant enrichment.

Results and Discussion

Numerous channelopathies reveal roles for bioelectrics in model systems

A number of studies have used gain-of-function approaches (misexpression of specific channel or pump proteins) to evaluate a role of bioelectric states in patterning processes such as development,[22,56,57] regeneration,[58,59] and tumor suppression/normalization.[31,60–68] Some studies also identified endogenous roles for bioelectrical gradients.[9,10,12,69,70] It is critical to identify the native conductances responsible for the salient bioelectrical prepatterns *in vivo* to place V_{mem} into pathways, understand the evolution of bioelectric control mechanisms, and provide candidate targets for biomedical intervention.

We searched databases of several popular model systems (mouse, zebrafish, *Drosophila*, and *C. elegans*) as well as literature, including human channelopathies, to identify known electrogenic genes with developmental phenotypes that include structural malformations. Tables 1–5 show channels, pumps, ion transporters, and gap junctions (and a few direct regulators of these) that are known to cause not just physiological disease conditions but also anatomical malformations (birth defects).

A large number of channelopathies were identified across taxa (Fig. 1A), with an outsize representation of channelopathies in the less complex organisms, particularly *Drosophila melanogaster* and *C. elegans* (Fig. 1B). While the large number of channelopathies identified may reflect the use of these model organisms in broad mutation screens (e.g., wing and bristle formation in *Drosophila,*[8] or length and girth in *C. elegans*[71]), it may also be the case that the large number of identified mutations in these species is due to smaller individual-to-individual variation than is seen in mammals, allowing for more narrowly defined ''normal'' phenotypes.

Channelopathies appear to primarily affect size and organization of tissues. The phenotypes created by channelopathies that we identified were mostly limited to alterations in size (31.6% of identified phenotypes), body patterning (i.e., left/right asymmetry, craniofacial patterning, limb patterning, etc., 31.9% of identified phenotypes), or tissue patterning (i.e., organ structure, 26.1% of identified phenotypes) (Fig. 1C). Due to variation in organ structure and function between species, we could not directly compare organs between all organisms, but we did detect a wide variety of organs affected in mammals (Fig. 1D). Craniofacial defects (14.7%), neural defects (16%), skeletal defects (12%), limb defects (10%), and heart defects (10%) were particularly common (Fig. 1D). These data reveal that numerous aspects of pattern formation, especially including the skeletal, neural, craniofacial, and cardiac systems, depend on the function of gene products that regulate bioelectric state.

Thus, the unexpected identification of ion channels in unbiased screens is a means by which many laboratories are brought into the field of bioelectricity. It should be noted that the lists in these Tables are a significant underestimate of the true prevalence of bioelectrical controls in development because single-gene knockouts/mutants are often masked by compensation and redundancy of functionality among channel family members or even completely different types of conductances.[72,73] Future work will examine the phenotypes of combinatorial knockouts and knock-ins of dominant negative proteins targeting entire subclasses of electrogenic proteins. Despite the difficulty of probing physiological mechanisms with gene targeting approaches, it is seen that classical genetic strategies have already revealed a striking number of bioelectric components in development of model systems with widely diverging developmental architectures, including man.

Table 1. Human Channelopathies

Protein (gene)	*UniProt number*	*Channel type*	*Mutant phenotype*	*Reference*
V-ATPase, (TCIRG1/VATB1)	Q13488/P15313	Vacuolar proton pump	Facial dysmorphism, dense bones	89,90
Kir3.2 (kcnj6)	P48542	Voltage-gated K^+ channel	Keppen-Lubinsky syndrome—craniofacial defects and microcephaly	91
K_v10.1 (kcnh1) and VATB2	O95259 and P21281	K^+ channel and vacuolar proton pump	Zimmermann-Laband and Temple-Baraitser syndrome—craniofacial and brain defects, dysplasia/aplasia of nails of thumb and great toe	92,93
GLRa4	Q5JXX5	Ligand-gated Cl^- channel	Craniofacial defects	94
K_{ir}6.1 (kcnj8)	Q15842	K^+ inwardly rectifying channel	Cantu syndrome—face, heart, skeleton, brain defects	95–97
NALCN	Q8IZF0	Na^+ leak channel	Freeman-Sheldon syndrome—congenital contractures of face and limbs, cerebral and cerebellar atrophy, small pituitary	98
CFTR	P13569	Cl^- channel transmembrane conductance regulator	Bilateral absence of vas deferens	99,100
SCN3A	Q9NY46	Voltage-gated Na^+ channel	Polymicrogyria	101
TRPV1, TRPV4	Q8NER1, Q9HBA0	Transient receptor potential cation channels	Temperature-induced face, heart defects	102
K_v3.1 (kcnc1)	P48547	Voltage-gated K^+ channel	Head/face dysmorphias	103
K_T3.2 (kcnk9)	Q9NPC2	K^+ two-pore domain channel	Birk-Barel dysmorphism syndrome—craniofacial defects, cortical patterning defects	104–106
K_{ir}6.2 (kcnj 11)	Q14654	Inwardly rectifying K^+ channel	Craniofacial defects, neural differentiation	107
K_v1.9 (kcnq1) (via epigenetic regulation)	P51787	Voltage-gated K^+ channel	Hypertrophy of tongue, liver, spleen, pancreas, kidneys, adrenals, genitalia	108–111
K_v1.9 (kcnq1)	P51787	Voltage-gated K^+ channel	Jervell and Lange-Nielsen syndrome—dysmorphism of inner ear	112–114
K_v3.3 (kcnc3)	O43525	Voltage-gated K^+ channel	Cerebellar dysplasia	56
K_{ir}2.1 (kcnj2)	P63252	Inwardly rectifying K^+ channel	Andersen-Tawil syndrome—craniofacial defects, abnormal limb patterning, gracile ribs, and long bones	115–117
Na_v1.2 (scn2a)	Q99250	Voltage-gated Na^+ channel	Laterality defects	118
Ca_v1.2 (cac1c)	Q13936	Voltage-gated Ca^{2+} channel	Timothy syndrome-webbed fingers, dysmorphic facial features, heart development defects, small teeth	119
Cx43 (gja1)	P17302	Gap junction	Heart defects (outflow tract and conotruncal), ODDD, visceroatrial heterotaxia	120–122

ODDD, oculodentodigital dysplasia.

Table 2. Mouse Channelopathies

Protein (Gene)	*UniProt number*	*Channel type*	*Mutant phenotype*	*Reference*
$K_{ir}7.1$ (kcnj13)	P86046	Inwardly rectifying K^+ channel	Cleft palate, delayed lung development	123
HCN1	O88704	Hyperpolarization-activated cyclic nucleotide-gated K^+ channel	Reduced brain size, loss of interneuron populations	124,125
CIC-3 (clcn3)	P51791	H^+/Cl^- exchange transporter	Brain patterning defects	126
$K_v3.1$ (kcnc1)	P15388	Voltage-gated K^+ channel	Growth deficits	124
TWIK-1 (kcnk1)	O08581	K^+ two-pore domain channel	atrial dilation	127
$K_v1.1$ (kcna1)	P16388	Voltage-gated K^+ channel	Megencephaly	128
$K_{ir}6.2$ (kcnj11)	Q61743	Inwardly rectifying K^+ channel	Craniofacial defects, negatively regulates neural differentiation	129
$K_v1.9$ (kcnq1) (via epigenetic regulation)	P97414	Voltage-gated K^+ channel	Hypertrophy of tongue, liver, spleen, pancreas, kidneys, adrenals, genitalia—Beckwith-Wiedemann syndrome; craniofacial and limb defects	108–110
$K_v1.9$ (kcnq1)	P97414	Voltage-gated K^+ channel	Jervell and Lange-Nielsen syndrome—dysmorphism of inner ear and limb, abnormalities in rectum, pancreas, and stomach	108,112–114,130,131
$K_v3.3$ (kcnc3)	Q63959	Voltage-gated K^+ channel	Cerebellar dysplasia (human), eye and wing defects (Drosophila)	56
$K_{ir}2.1$ (kcnj2)	P35561	Inwardly rectifying K^+ channel	Andersen-Tawil syndrome—craniofacial defects (narrow maxilla, cleft secondary palate), abnormal limb patterning, gracile ribs, and long bones	115–117,132
GABA-A receptor (gabrb3)	P63080	Ligand-gated Cl^- channel	Angelman syndrome—cleft palate, cerebellar vermis hypoplasia, abnormal cochlear development and morphology	133–137
ANO1	Q8BHY3	Ca^{2+}-activated Cl^- channel	Tracheomalacia with cartilage ring defects, abnormal trachealis muscle development	138
$K_{ir}3.2$ (kcnj6)	P48542	G-protein coupled inwardly rectifying K^+ channel	Cerebellar development defects	139–142
$K_v11.1$ (kcnh2)	O35219	Voltage-gated inwardly rectifying K^+ channel	Cardiac, craniofacial patterning defects	143
$K_vb1.3$ (kcnab1)	P63143	Voltage-gated K^+ channel subunit	Cardiac hypertrophy	144
5-HT3B (htr3b)	Q9JHJ5	Ligand-gated cation channel	Increased bone density and body length in females, decreased bone density and body length in males	145
CIC-2 (clcn2)	Q9R0A1	Voltage-gated Cl^- channel	Abnormal brain and eye morphology	146
CIC-5 (clcn5)	Q9WVD4	H+/Cl^- exchange transporter	Renal tubular defects, kyphosis, abnormal tooth development	147
nAChRα7 (chrna7)	P49582	Ligand-gated cation channel	Abnormal bone structure, abnormal cerebral cortex morphology, abnormal myeloblast development	148–150

(*continued*)

TABLE 2. (CONTINUED)

Protein (Gene)	*UniProt number*	*Channel type*	*Mutant phenotype*	*Reference*
AchR (chrng)	P04760	Ligand-gated cation channel	Abnormal skeletal muscle morphology, abnormal neuromuscular junction morphology	151
Cx50 (gja8)	P28236	Gap junction	Abnormal lens development, micropthalmia	152,153
Cx45 (gjc1)	P28229	Gap junction	Cardiac defects (cushion patterning) and impaired hematopoiesis	154–157
Cx43 (gja1)	P23242	Gap junction	Deficits in myogenesis, abnormal osteoblast differentiation, left/right asymmetry randomization, heart defects (outflow tract and conotruncal), neural tube defects, delayed ossification of clavicles, ribs, vertebrae, and limbs, syndactyly and limb defects, craniofrontonasal syndrome	158–164
Cx37 (gja4)	P28235	Gap junction	Lymphatic system patterning	165,166
Cx26 (gjb2)	Q00977	Gap junction	Cochlear development defects	167
Cx40 (gja5)	Q01231	Gap junction	Malformed bone in wrists, digits, and sternum joints	168
PANX3	Q8CEG0	Gap junction	Delayed hypertrophic chondrocyte and osteoblast differentiation and delayed initiation of bone mineralization	169
NMDAR2D (grin2d)	O15399	Ligand-gated cation channel	Abnormal bone mineralization and structure, reduced heart size	IMPC[a]
GLRB	P48168	Ligand-gated Cl^- channel	Abnormal vertebral column morphology and abnormal intervertebral disk morphology	170
$K_{ir}7.1$ (kcnj13)	P86046	Inwardly rectifying K^+ channel	Cleft palate, abnormal lung development, abnormal tracheal development	123,171
SCNN1B	Q9WU38	Sodium-permeable, nonvoltage-sensitive Na^+ channel	Abnormal pelvic girdle bone morphology, decreased rib number, abnormal kidney morphology	IMPC[b] 172
$Ca_v1.2$ (cacna1c)	Q01815	Voltage-gated Ca^{2+} channel	Abnormal brain morphology, enlarged lateral ventricles, cardiac hypertrophy	173,174

[a]https://www.mousephenotype.org/data/genes/MGI:95823
[b]https://www.mousephenotype.org/data/genes/MGI:104696

Electrogenic proteins are an ancient common factor in regeneration across Kingdoms

Regeneration is a process that implements morphogenesis in complex body organs or appendages. It is similar to development, except that unlike embryogenesis, which always begins with the same reliable state (fertilized egg), regeneration builds species-specific target morphologies from diverse starting states (injury conditions with variable amounts and locations of missing tissue). A critical tissue in all instances of regeneration is the blastema—early cells at the site of injury, which must make decisions about differentiation, proliferation, and spatial patterning that determine the fate of the wound (scarring or functional regeneration). We thus used bioinformatics to compare published transcriptomic analyses of transcriptional changes occurring in regeneration blastemas (Fig. 2A). We specifically sought to compare extremely distant taxa (crossing Kingdoms of life), to identify components that were associated with regeneration *per se*, and not the specifics of any one body-plan architecture or physiological/ecological lifestyle.

Common to animal regeneration (planarian body fragments, frog limb, axolotl limb, and deer antler) were 10

Table 3. Zebrafish Channelopathies

Protein (gene)	*UniProt number*	*Channel type*	*Mutant phenotype*	*Reference*
PANX3	E7F7V4	Gap junction	Delayed hypertrophic chondrocyte and osteoblast differentiation and delayed initiation of bone mineralization	169
$Na_v1.4a$ (scn4aa)	A0A0R4IJX4	Voltage-gated Na^+ channel	Abnormal caudal fin structure, small head and trunk, disorganized skeletal muscle	175
$Na_v1.5$ (scn12aa)	F1R3Q5	Voltage-gated Na^+ channel	Abnormal cardiac ventricle and atrium morphology	176,177
GluR2A (gria2a)	A0A0R4ING5	Ligand-activated cation channel	Abnormal cranial cartilage, achondrogenesis, absent ethmoid cartilage, enlarged fourth ventricle	178
SLC8A4A	A4UQV6	Ca^{2+}/Na^+ antiporter	Decreased length, abnormal digestive tract development, heart mislocalized abnormal liver development	179,180
SLC24A5 (nckx5)	B0V3S7	$Na^+/K^+/Ca^{2+}$ exchanger	Delayed development of melanin pigmentation (''golden'' phenotype)	181
SLC26A2	E7F9I7	So^{2-} transporter	Defective otolith patterning, abnormal semicircular canal morphology	182
MCU	F1QT29	Ca^{2+} uniporter	Abnormal anterior/posterior axis specification; abnormal cell migration during gastrulation, abnormal notochord	183
CACNB2	B2XY76	Voltage-gated Ca^{2+} channel	Small cardiac ventricle, heart is malformed and edematous, fragile heart tube	184
P2RX3A	B3DG55	ATP-gated cation channel, purinoceptor	Hypotrophic ceratobranchial cartilage, abnormal ceratohyal cartilage, pharyngeal and ventral mandibular arches malformed	185
PIEZO1	E7FD74	Mechanosensitive cation channel	Small head, caudal fin curled, erythrocyte deformities	186,187
SLC8A1	Q32SG8	Ca^{2+}/Na^+ antiporter	Small head, heart abnormalities	188,189
CLIC6	A0A286YBT4	Cl^- intracellular channel	Abnormal otolith morphology, hydrocephalus, left/right defects, and curved body axis	190
TASK1 (kcnk3)	Q5TZ59	K^+ leak channel	Abnormal heart morphology	191
TASK2 (kcnk5)	A0A2R8PYU3	K^+ two-pore domain channel	Long anal fin; abnormal caudal fin	12
CNGA2A (cnga5)	Q0GFG2	Cyclic nucleotide-gated cation channel	Malformed otolith, right/left symmetry defects	192
$K_v2.1$ (kcnb1)	A0A2R8Q685	Voltage-gated K^+ channel	Small fourth ventricle; disrupted gastrulation	193
Kir4.1 (kcjn10)	E7FD27	Inwardly rectifying K^+ channel	Swim bladder absent, pronephric duct dilated	194
$Ca_v1.2$ (cacna1c)	Q5TZF1	Voltage-gated Ca^{2+} channel	Timothy syndrome, hydrocephalus; abnormal heart morphology, small heart, dilated pronephridic duct, cystic kidney, abnormal mandibular arch	195–197
TRPC1	E1U7G1	Transient receptor potential cation channel	Microphthalmia; disrupted angiogenesis, increased curvature in postvent region	198
Kir7.1 (kcnj13)	Q0KIZ7	Inwardly rectifying K^+ channel	Pigmentation issues on anal and caudal fins	199,200

(*continued*)

TABLE 3. (CONTINUED)

Protein (gene)	*UniProt number*	*Channel type*	*Mutant phenotype*	*Reference*
MagT1	Q7ZV50	Mg^{2+} transporter	Small, malformed head	201
H^+ V-ATPase	Multiple	Proton pump	Left–right asymmetry defects, muscle and nerve repair	58,76
CFTR	A0A0R4ID63	cAMP-dependent Cl^- channel	Primordial germ cell development	202
Cx41.8 (gja5)	F1QL21	Gap junction	''*leo*'' phenotype, pigmentation pattern defects	203,204
Cx39.4 (*luchs*)	Q1LWG0	Gap junction	Loss of trunk striping, pigmentation pattern defects	203
Cx43 (gja1)	O57474	Gap junction	Small fin size, failure of joint morphogenesis, and abnormal pattern regulation	205–207
FXYD6	F1QK04	Na^+/K^+ ATPase channel modulator	Abnormal Meckel's and ceratohyal cartilage, small head, abnormal skeletal muscle	208

TABLE 4. *DROSOPHILA* CHANNELOPATHIES

Protein (gene)	*UniProt number*	*Channel type*	*Misexpression phenotype*	*Reference*
LD30634p (ATP6AP2)	Q9VHG4	V-ATPase proton pump	Abnormal wing hair and bristle patterning, pigmentation and brain patterning, small size, small head size, blistered wings	90,209–211
BEST1	Q9V3J6	Ca^{2+}-activated Cl^- channel	Bifurcation of posterior crossvein	8
BEST2	Q9VRW4	Ca^{2+}-activated Cl^- channel	Wings small and severely malformed	8
BEST3	Q9VUM7	Ca^{2+}-activated Cl^- channel	Small narrow wings (male), missing anterior and incomplete posterior crossover vein, L2 vein bifurcated	8
BIB	P23645	Nonselective cation channel, aquaporin	Defects in neural development, hyperplasia of neuroblasts, sensillum precursors and peripheral glia, small wing size, failure of heart differentiation, increased macrochaetae and supernumary bristles, notum malformation and color defects	48,212–215
BRV2	M9PFT4	Transient receptor potential channel	Bifurcation of posterior crossvein	8
GluClα	Q94900	Glutamate-gated Cl^- channel	Bristle defects	8
GluRIIB	Q9VMP3	Ionotropic glutamate receptor	Bifurcation of posterior crossvein	8
GPHR	Q3ZAN1	Voltage-gated Cl^- channel	Abnormally small body and wing blades	216
iINAF-A; B; C	A8JUT0, A8WH7, Q6IIF2	Transient receptor potential channel modulator	Bifurcation of posterior crossvein	8
INX2	Q9V427	Gap junction	Small eye size, failure of epithelial patterning, loss of bristles, bristle morphology defects, abnormal foregut development, failed germline differentiation, and spermatogenesis	48,217–221
INX3	Q9VAS7	Gap junction	Cuticle defects, and irregular denticle belts, loss of epithelial organization, polarity defects in epidermis, dorsal closure defects, incomplete formation of posterior crossvein and L5 vein, bifurcation of L4 and L5 veins	219,222
INX4	Q9VRX6	Gap junction	Failure of germline differentiation and spermatogenesis	221

(*continued*)

TABLE 4. (CONTINUED)

Protein (gene)	*UniProt number*	*Channel type*	*Misexpression phenotype*	*Reference*
IR67A	Q9VT09	Ionotropic glutamate receptor	Thick veins, bifurcation of posterior crossvein, and L3 vein	8
IR76A	Q9VW39	Ionotropic receptor	Incomplete posterior crossvein, bifurcated L5 vein	8
IR7B	Q9W3P4	Ionotropic receptor	Incomplete or bifurcated posterior crossvein, bifurcated L5 vein	8
Ir84a	Q9VIA5	Ionotropic glutamate receptor	Thick veins, bifurcated posterior crossvein	8
Ir92a	Q9VDN3	Ionotropic glutamate receptor	Bristle defects, abnormal vein pigment	8
Ir94g	Q9VCM1	Ionotropic receptor	Bristle defects, abnormal vein pigment	8
Ir94h	Q9VCM0	Ionotropic receptor	Bristle defects	8
$K_{ir}2.1$ (Irk1)	Q95UP7	Inwardly rectifying K^+ channel	Thick veins, loss of anterior crossvein, L5 and L4 bifurcation, notum malformation, bristle morphology defects	8,48
$K_{ir}2.2$ (Irk2)	Q8WQ82	Inwardly rectifying K^+ channel	Wing patterning defects, bristle defects, L5 and L4 bifurcations, loss of anterior crossvein, thick veins	116
$K_{ir}2.3$ (Irk3)	X2JAW9	Inwardly rectifying K^+ channel	Small wings, severe wing vein defects L5 and L4 bifurcations, loss of anterior crossvein, thick veins	116
JYα	A8QI34	Cation-transporting P-type ATPase	Defects in spermatogenesis and sperm motility	223
KCNQ	Q8IT87	Voltage-gated K^+ channel	Slow rate of development, enclosure failure, abnormal heart function, posterior crossvein bifurcation	111,224
α1U (na)	Q8I877	Na^+ leak channel	Small size, long cylindrical abdomen, bristle defects, ectopic vein, notum malformation	8,48,225
nAChRα5 (CHRNA5)	Q8T5F5	Ligand-gated cation channel	Bifurcated posterior crossvein, notum malformation	8,48
nAChRα6 (CHRNA6)	M9PFD8	Ligand-gated cation channel	Bifurcated posterior crossvein	8
nAChRα7 (CHRNA7)	Q86MN7	Ligand-gated cation channel	Bifurcated posterior crossvein	8
NaCP60E	Q9W0Y8	Voltage-gated Na^+ channel	Bifurcated posterior crossvein, pigment abnormality	8
Nan	Q9VUD5	Transient receptor potential channel	Incomplete or bifurcated L5 wing vein	8
Nhe2	Q9NGZ4	Na^+/H^+ exchanger	Epithelial patterning, abnormal gut morphology, defects in fat body development, defects in eye morphology	93,226
nrv2	Q24048	Na^+/K^+-transporting P-type ATPase	Cardiac lumen collapse, defective blood–brain barrier formation, tracheal tube size defects, bristle loss	48,227,228
Ogre	P27716	Gap junction	Small, disorganized optic lobes	229
olf186-F	Q9U6B8	Ca^{2+} release-activated Ca^{2+} channel	Small body size, wing defects, abnormal abdominal dorsal multidendritic neurons	230–232
Or47a	P81921	Ligand-gated cation channel	Posterior crossvein bifurcation	8
ppk	O44940	Degenerin/epithelial Na^+ channel	Large body size, bifurcated posterior crossvein	8,233
ppk17	Q9VJI4	Degenerin/epithelial Na^+ channel	Bifurcated posterior crossvein, L2 vein, and L3 vein	8
ppk25	A1Z6S4	Degenerin/epithelial Na^+ channel	Bifurcated posterior crossvein and L5 vein	8

(*continued*)

TABLE 4. (CONTINUED)

Protein (gene)	*UniProt number*	*Channel type*	*Misexpression phenotype*	*Reference*
ppk30	Q9VAJ5	Degenerin/epithelial Na^+ channel	Bifurcated L4 and L5 veins, incomplete posterior crossvein and L5 vein	8
Rdl	P25123	GABA-gated Cl^- channel	L2 incomplete, ectopic bristles, pigment defect	8
rpk	O46342	Degenerin/epithelial Na^+ channel	Small wings, incomplete L5 formation, bifurcation of L4 and L5 veins	8,234
SERCA	Q8STG9	Ca^{2+}-transporting P-Type ATPase	Ectopic veins, ectopic bristles, pigment defect, cardiac dilation, wing notches, malformed legs, reduced eye number, abnormal eyes	8,235,236
sh	P08510	Voltage-gated K^+ channel	Abnormal pigmentation, abnormal wing expansion, abnormal abdominal muscles, head eversion defects, foreshortened wings and legs, bifurcated posterior crossvein	8,237,238
SLO2	A8DY93	Ca^{2+}-activated K^+ channel	Incomplete posterior crossvein	8
Stim	P83094	CRAC channel regulator	Loss of bristles, hair cell duplication, small larval size, small abnormal eyes, notched wings, small wings, blistered wings, ectopic wing veins	8,48,232,239
Task6	Q9VFS9	Two-pore domain K^+ channel	Bifurcated posterior crossvein, notum malformation	8,48
Teh1	Q9VH54	Voltage-gated Na^+ channel	Black spots on wing below L5 vein	8
THADA	Q9VWB9	sarco(endo)plasmic reticulum Ca^{2+}-ATPase regulator	Gain/loss of bristles, malformed notum	48
TRPM	A8DYE2	Transient receptor potential channel	Decreased cell size, small salivary glands, shortened malpighian tubules	240,241
Trpml	Q9VW35	Transient receptor potential channel	Reduced neuromuscular junction boutons, crumpled wings, gain of bristles, notum malformation	48,242,243
unc79	Q06AJ1	Na^+ leak channel complex regulator	Bifurcated posterior crossvein, cylindrical abdomen	8,225
unc80	Q9VB11	Na^+ leak channel complex regulator	Bifurcated posterior crossvein, ectopic veins, pigment defects	8
wtrw	Q9VHY7	Transient receptor potential channel	Incomplete posterior crossvein	8
CG18549	Q9VG64	Ion channel regulatory protein	Posterior crossover vein bifurcation, bristle morphology defects, notum malformation	8,48

CRAC, calcium release-activated channel; TRP, transient receptor potential channel.

TABLE 5. *CAENORHABDITIS ELEGANS* CHANNELOPATHIES

Protein (gene)	*UniProt number*	*Channel type*	*Mutant phenotype*	*Reference*
acr-2	P48182	Ligand-gated cation channel	Increased length and girth, abnormal gonad morphology	71
acr-6	Q9N4M3	Ligand-gated cation channel	Increased girth	71
acr-7	P45963	Ligand-gated cation channel	Increased length	71
acr-9	Q18556	Ligand-gated cation channel	Reduced girth	71
acr-10	Q21645	Ligand-gated cation channel	Increased girth	71
acr-14	Q22224	Ligand-gated cation channel	Increased girth	71
acr-15	O16926	Ligand-gated cation channel	Reduced girth and length	71
acr-18	G5EG72	Ligand-gated cation channel	Reduced girth and length	71
acr-19	B3WFZ2	Ligand-gated cation channel	Decreased body length and increased girth	71

(*continued*)

TABLE 5. (CONTINUED)

Protein (gene)	*UniProt number*	*Channel type*	*Mutant phenotype*	*Reference*
acr-21	A0A3P6MY71	Ligand-gated cation channel	Increased girth	71
acr-23	G5EG88	Ligand-gated cation channel	Increased girth	71
che-6	O61827	Cyclic nucleotide-gated channel	Abnormal sensillum morphology	244
eat-4	P34644	Glu/Na^+ symporter	Abnormal pharynx morphology	245
eat-6	P90735	Na^+/K^+ ATPase	Abnormal sarcomere morphology, decreased girth and body length, abnormal pharynx	245–247
egl-2	A0A0K3AVF4	Voltage-gated K^+ channel	Increased length and girth, abnormal chemosensory neurons	71,248
egl-19	Q8MQA1	Voltage-gated Ca^{2+} channel	Variable body length, decreased girth, blocked anus, tail morphology defects, pigmentation defects	71,245,246,249–251
egl-23	C0Z3L1	K^+ two-pore domain channel	Decreased body length and increased girth	71,246
egl-36	G5EFC3	Voltage-gated K^+ channel	Increased body length and girth	71
exc-4	Q8WQA4	Voltage-gated Cl^- channel	Defects in excretory canal, pigmentation defects	252
exp-2	H2KZQ6	Voltage-gated K^+ channel	Abnormal pharyngeal muscles, pharyngeal disorganization	246,253,
flr-1	G5EGI5	Degenerin/epithelial Na^+ channel	Pigmentation defects, reduced body length, reduced girth	71,249
lev-1	Q27218	Ligand-gated cation channel	Reduced girth and body length	71
lev-8	Q93329	Ligand-gated cation channel	Increased body length and girth	71
lov-1	Q09624	Transient receptor potential channel	Increased girth	71,254
mec-10	P34886	Epithelial Na^+ channel	Variable body length and increased girth	71
mod-1	Q9GQ00	Ligand-gated Cl^- channel	Increased body length and girth	71
unc-77	V6CKM5	Na^+ leak channel	Decreased body length and girth	71
ocr-3	Q22374	Transient receptor potential channel	Increased girth	71
ocr-4	Q9N3Y9	Transient receptor potential channel	Decreased body length and increased girth	71
osm-9	G5EBV8	Transient receptor potential channel	Reduced girth and decreased body length, abnormal uterine seam cells	71,255
sup-9	O17185	K^+ two-pore domain channel	Increased girth and length	71
tax-4	Q03611	Cyclic nucleotide-gated channel	Failure of left/right asymmetric neuronal fate specification, abnormal sensory neurons	256,257
trp-1	P34586	Transient receptor potential channel	Increased girth	71
trp-2	Q8I6Y9	Transient receptor potential channel	Decreased body length and increased girth	71
trp-4	Q9GRV5	Transient receptor potential channel	Increased girth	71
unc-110	Q18120	Outwardly rectifying K^+ channel	Reduced girth	71
unc-2	A0A3B1E663	Voltage-gated Ca^{2+} channel	Reduced girth and length, abnormal axon branching, failure of left/right asymmetric neuronal fate specification	71,246,248,258

(*continued*)

TABLE 5. (CONTINUED)

Protein (gene)	*UniProt number*	*Channel type*	*Mutant phenotype*	*Reference*
unc-7	Q03412	Gap junction	Variable body width, short body length	71
unc-8	Q21974	Epithelial stretch-gated Na^+ channel	Reduced girth and body length, swollen ventral nerve cord	71,259
unc-9	O01393	Gap junction	Small male fan, short body length, reduced girth	71
unc-17	P34711	VAChT	Reduced body size and girth	246,260
unc-32	P30628	V-Type ATPase	Abnormal body wall muscle morphology, pigmentation defects, small size and increased girth, abnormal pharynx, narrow rachis	71,245,246,261
unc-36	P34374	Voltage-gated Ca^{2+} channel	Increased length, reduced girth, loss of left/right asymmetry	245,246,262
unc-38	Q23022	Ligand-gated cation channel	Reduced girth and decreased body length	71
unc-49	G5ECD3	Ligand-gated Cl^- channel	Reduced body size	263
unc-58	Q22271	K^+ two-pore domain channel	Reduced body length and girth	264,265
unc-63	Q9N587	Ligand-gated cation channel	Decreased body length and increased girth	71
unc-68	A0A2C9C3E8	Ca^{2+} release channel	Reduced girth and body length, abnormal pharyngeal axons	71,266
unc-77	V6CKM5	Na^+ leak channel	Reduced girth, decreased body length. Abnormal vulva morphogenesis	71,267
unc-80	Q9XV66	Na^+ leak channel	Small eggs	268
unc-103	G5EFJ9	Voltage-gated K^+ channel	Reduced girth, variable body length, abnormal sarcomere morphology, abnormal body wall musculature	71,265,268
unc-105	Q09274	Epithelial Na^+ channel	Animals are shorter and thinner, abnormal body wall musculature, abnormal body morphology, protruding vulva	71,246,265
trpa-1	Q18297	Transient receptor potential channel	Variable body length and increased girth	71
delm-1	O45402	Degenerin/epithelial Na^+ channel	Reduced girth and decreased body length	71
trpa-2	Q21517	Transient receptor potential channel	Increased girth and decreased body length	71
acc-4	Q9U358	Ligand-gated Cl^- channel	Reduced girth and body length	71
asic-2	Q22851	Epithelial Na^+ channel	Decreased body length and increased girth	71
egas-3	Q9XTS9	Epithelial Na^+ channel	Abnormal body proportions	71
egas-2	Q9U1T8	Epithelial Na^+ channel	Reduced girth and body length	71
del-9	Q18077	Acid-sensing ion channel	Abnormal body proportions	71
delm-2	P91103	Degenerin/epithelial Na^+ channel	Reduced girth and body length, abnormal ventral nerve cord patterning	71,269
acd-2	P91100	Degenerin/epithelial Na^+ channel	Reduced girth	71
del-7	Q18651	Epithelial Na^+ channel	Decreased body length	71
acd-5	O01664	Degenerin/epithelial Na^+ channel	Reduced girth and body length compared	71
asic-1	O01635	Epithelial Na^+ channel	Reduced girth and body length	71

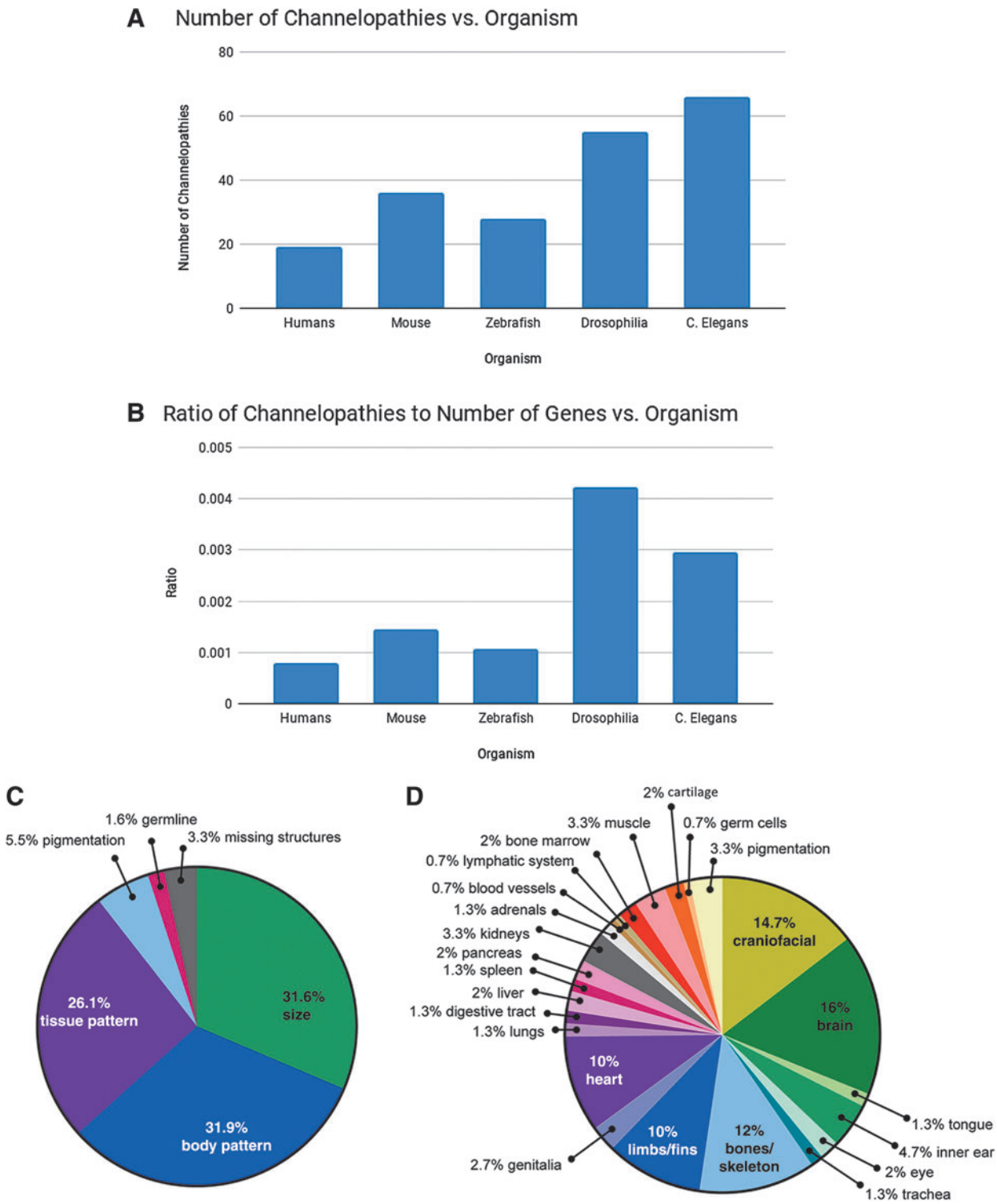

FIG. 1. Channelopathies across model systems. **(A)** The number of known morphogenetic phenotypes arising from ion channel mutations (as obtained from their respective databases) is shown for human, mouse, zebrafish, fruit fly, and nematode models. These data reflect possible differences in the density with which each model system's genome has been examined for anatomical channelopathies. **(B)** The ratio of channelopathies per total number of genes in each organism is shown; plotting the number of morphogenetic channelopathies relative to the genome size enables estimates of the size-corrected prevalence of ion channel genes that impact anatomy. The disproportionate number of anatomical channelopathies found in *Drosophila* may suggest that its genome is especially reliant on ion channels for patterning, or could be due to higher density of analysis having been done in the fruit fly model system. **(C)** Channelopathy phenotypes were broadly categorized, and relative proportions are compared in a pie chart. The majority of developmental channelopathies affect size or patterning, although changes to pigmentation, germline mutations, and missing structures were also identified. **(D)** Tissue-specific channelopathy phenotypes were considered in combined rodent and human models, and the relative proportion of tissue-specific effects were compared. Brain, heart, and craniofacial defects were most commonly affected by ion channel mutations, with limb and skeletal defects also prevalent. The disproportionate representation of brain, heart, face, and limb defects in channelopathies suggests that ion channels play an important role in patterning of these organs.

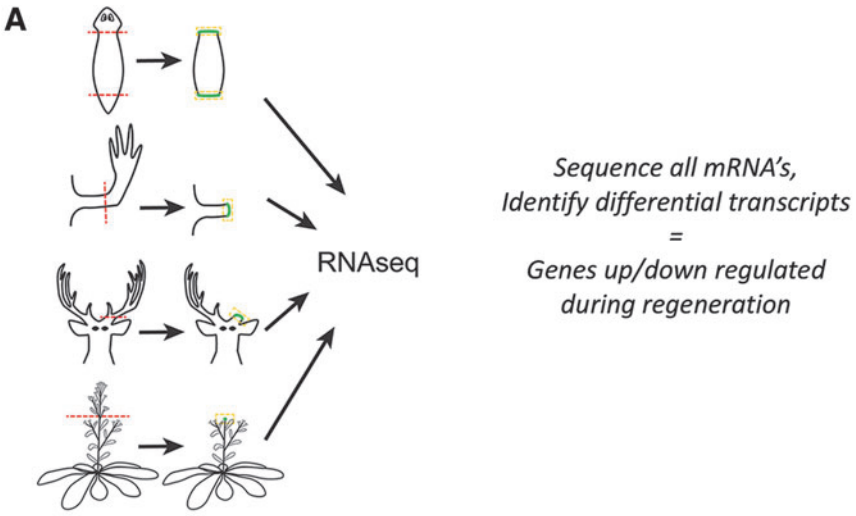

B Transcripts significantly regulated in regeneration

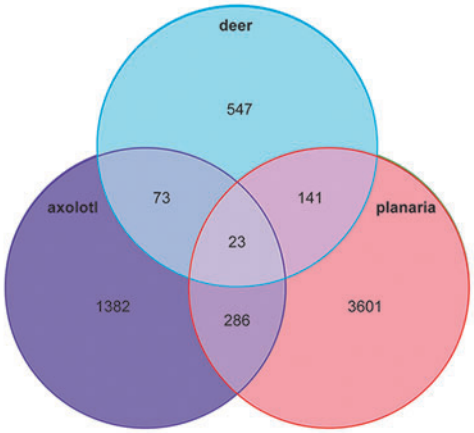

B'

LARS	leucyl-tRNA synthetase
STARD10	StAR related lipid transfer domain containing 10
PLK4	polo like kinase 4
CCNB3	cyclin B3
POLA1	DNA polymerase alpha 1, catalytic subunit
DPP10	dipeptidyl peptidase like 10
GRN	granulin precursor
TPM1	tropomyosin 1
PSAP	prosaposin
ATP6V1B2	**ATPase H+ transporting V1 subunit B2**
NAGA	alpha-N-acetylgalactosaminidase
CTSB	cathepsin B
ITGB2	integrin subunit beta 2
SLC12A9	solute carrier family 12 member 9
SYNGR2	synaptogyrin 2
PI15	peptidase inhibitor 15
MYO5A	myosin VA
CLCN7	**chloride voltage-gated channel 7**
CD151	CD151 molecule (Raph blood group)
ATP6V0C	**ATPase H+ transporting V0 subunit c**
SLC37A2	solute carrier family 37 member 2
PLD3	phospholipase D family member 3
DGAT2	diacylglycerol O-acyltransferase 2

C Transcripts significantly regulated in regeneration

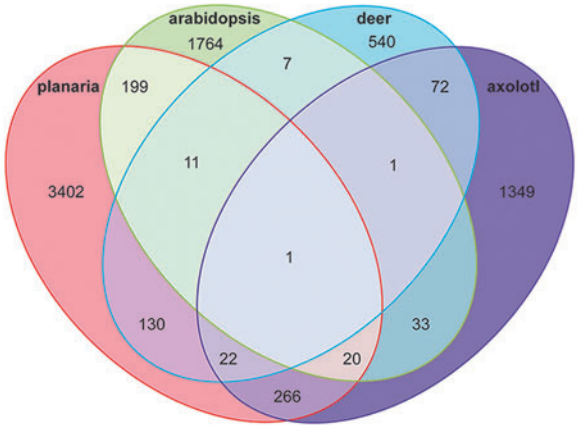

C'

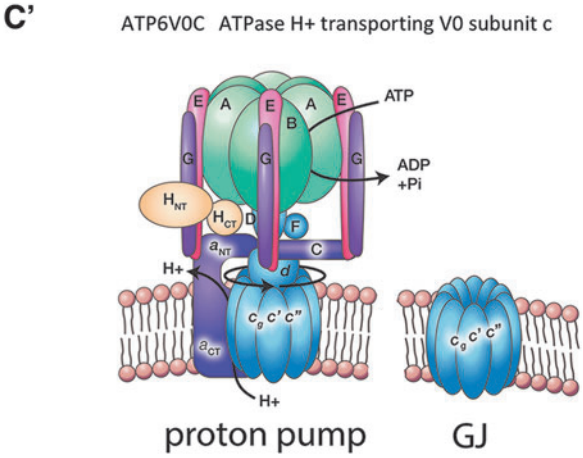

FIG. 2. Bioelectric signature of transcriptional profile in regeneration. **(A)** A schematic representation of the analysis performed: published transcriptomic profiles of regeneration blastemas from planaria, axolotl, deer antlers, and plants (*Arabidopsis*) were compared to determine common DEGs across these highly diverse samples. **(B)** Twenty-three differentially expressed genes are common to regeneration among taxa as diverse as mammals (deer antlers), amphibians (axolotl), and invertebrate flatworms (planaria). These are listed in **(B′),** and include two subunits of the proton pump complex and a voltage-gated chloride channel. **(C)** Remarkably, when a plant (*Arabidopsis*) dataset is included, only one DEG is common in regeneration across Kingdoms, and thus across independent origins of multicellularity: an evolutionarily ancient and highly conserved protein that is a key subunit of both, the V-ATPase proton pump and gap junctions (**C′**), which have both been implicated in regeneration, wound healing, and developmental patterning.[58,74,77,78,205,270–277] DEGs, differentially expressed genes.

Table 6. Transcripts Common to Blastemas Across Kingdoms

Gene name	*Type of protein*
POLA1	DNA polymerase alpha 1, catalytic subunit
DPP10	Dipeptidyl peptidase like 10
GRN	Granulin precursor
TPM1	Tropomyosin 1
PSAP	Prosaposin
CTSB	Cathepsin B
ITGB2	Integrin subunit beta 2
CD151	CD151 molecule (Raph blood group)
ATP6V0C	ATPase H^+-transporting V0 subunit c
PLD3	Phospholipase D family member 3

transcripts listed in Table 6 and Figure 2B. These 10 genes define a regenerative signature across regeneration modes, including those based on adult stem cells, dedifferentiation, and tissue renewal.

Remarkably, when crossreferenced with transcriptomes from plant (*Arabidopsis*) regeneration, one common gene remains: the transmembrane ring protein component of the proton-transporting V-ATPase (Fig. 2C). This fascinating structure is related to both gap junctions (a.k.a., electrical synapses)[74] and ion pumps that polarize cells, and has already been functionally implicated in embryonic left–right patterning in chick, zebrafish, and frog,[75,76] zebrafish eye morphogenesis,[77] frog tail regeneration,[58] wound healing in *Drosophila,*[78] and stem cell regulation in the mouse brain.[79] In some of these cases (e.g., chick and frog), the V-ATPase pump is known to function on the cell surface, generating a significant hyperpolarization of cells by the efflux of positive charges.[58,76,80] It is also a regulator of pH, at both the cellular and organelle level,[81] and the conserved c subunit has been proposed to function as a gap junction.[74,82–86]

It is a remarkable fact that an ancient precursor to widely conserved proteins that set resting potential (ion pumps) and distribute it across tissue networks (gap junctions) is the one common factor in regeneration across Kingdoms. Moreover, because of the distinct origins of multicellularity in plants and animals, it is interesting to note that evolution pressed this highly versatile protein complex into service for tissue regeneration at least twice independently. This finding is consistent with the central importance of bioelectrical cellular states and communication in regenerative patterning processes.

V_{mem} differences among normal and transformed cell types in human and rodents

Seminal work by Binggeli and Weinstein[41] building on the work of Cone[27,28,87,88] hypothesized that resting membrane potential, V_{mem}, predictably varied across cell types according to cell type and cell cycle stage. They performed a meta-analysis of literature that reported V_{mem} in a variety of cell types and stages, showing that proliferative cells and cancer cells both were more depolarized than differentiated cells, and that a boundary existed at around −36 mV that differentiated proliferating and nonproliferating cells.[41]

Binggeli and Weinstein were only able to find V_{mem} values for a few examples in each cell type, however, in the ensuing 34 years electrophysiological determination of V_{mem} has become a standard laboratory practice, providing ample examples for further assessment of V_{mem} as a function of cell cycle state. Thus, we revisited the Binggeli and Weinstein study,[41] and analyzed all of the V_{mem} measurements we could find in a thorough literature search. We found V_{mem} values for 41 cancer cell types across 3 species from 18 publications and V_{mem} values for 70 noncancer cell types across 9 species from 24 publications (Supplementary Table S1). Our list did also include the publications described in Binggeli and Weinstein.[41]

We found that V_{mem} was generally more hyperpolarized in normal differentiated tissues than in their cancerous counterparts for both rodent and human tissues (Fig. 3A), a finding consistent with the conclusions in Binggeli and Weinstein. A meta-analysis using a random-effects model comparing data which had both cancer and somatic tissue V_{mem} values in the same study showed a significant decrease in V_{mem} in

FIG. 3. Meta-analysis of bioelectric data in cancer. **(A)** Violin plots show membrane potential (V_{mem}) values for somatic and cancerous tissues in human and rodent cell types. Rodent cancerous cells were significantly more depolarized than somatic cells (95% CI for change in voltage: −30.3 to −11.2, $p<0.0001$), but V_{mem} in human cells overall was not significantly different in somatic and cancerous cells. Data were collected from reports in the literature (Supplementary Table S1) and analyzed by meta-regression. Papers that contained values for both somatic and cancerous tissues are shown as paired, with a line connecting the values. When only considering paired samples, a random-effects model found that somatic cells were significantly more hyperpolarized than cancerous cells derived from the same cell type. For human somatic cells, the average was 16 mV more hyperpolarized than comparable cancer cells (95% CI: 1.1–30.8, $p=0.0343$). Rodent somatic cells were on average 32.3 mV more hyperpolarized than the corresponding cancer cells (95% CI: 8.8–55.7, $p=0.0068$). Heterogeneity between the studies was significant ($p<0.05$) for both human and rodent studies. $*p<0.05$, $**p<0.01$. **(B)** There is an inverse relationship between the V_{mem} of somatic cells and the amount of change between the somatic and cancerous cells of the same type, suggesting that cells that start more hyperpolarized have larger increases in depolarization than those that start with V_{mem} closer to 0. A mixed-effects model identified this relationship as significant, with a 0.85-fold reduction in V_{mem} change for every 1 mV change in the somatic V_{mem}. $p<0.0001$. **(C, D)** When considered in broad tissue-specific categories, the majority of cancerous cells appear to be more depolarized than the somatic tissues from which they are derived in rodent model systems (**C**) and human model systems (**D**). In this analysis, only data for which both somatic and cancerous cell types were represented in our dataset could be used, (grey shaded data in Table 7 for human cells and 8 for rodents) resulting in an insufficient number of studies that could be included in a meta-analysis. Thus, we were unable to determine the significance of this relationship. **(E–H)** Data were grouped into broad categories to show the types of somatic (**E, G**) and cancer (**F, H**) tissues from which we were able to collect V_{mem} values in both human and rodent model systems. CI, confidence interval.

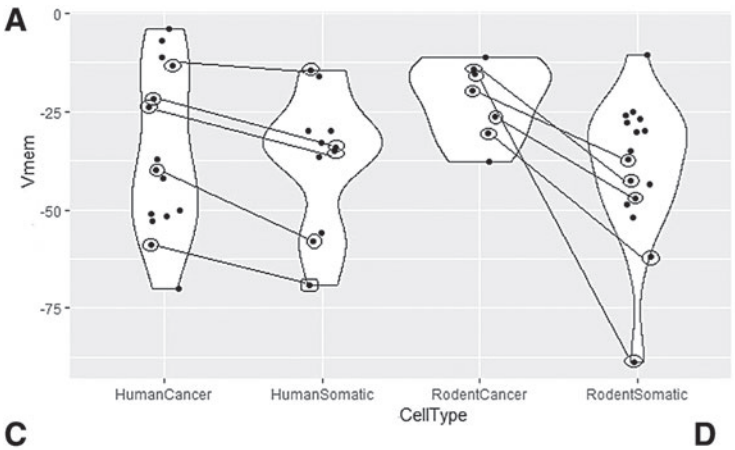
A
Vmem
0
-25
-50
-75
HumanCancer
HumanSomatic
RodentCancer
RodentSomatic
CellType

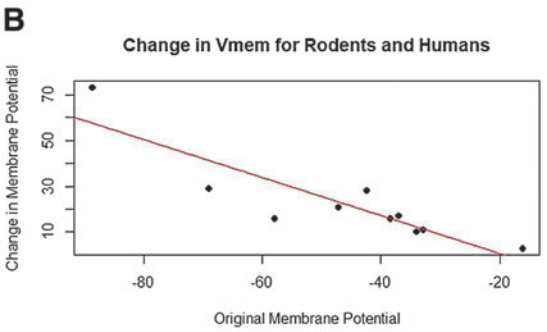
B
Change in Vmem for Rodents and Humans
Change in Membrane Potential
70
50
30
10
-80
-60
-40
-20
Original Membrane Potential

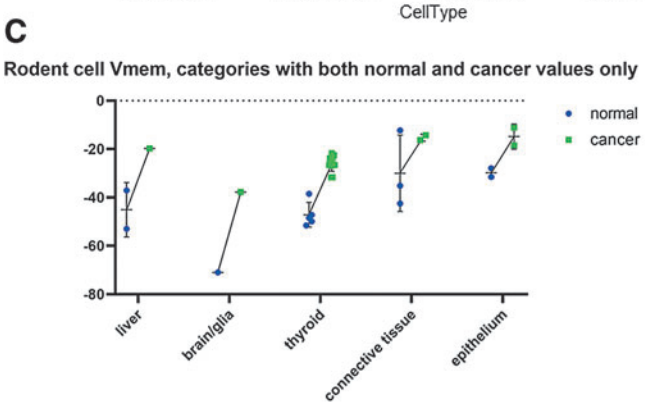
C
Rodent cell Vmem, categories with both normal and cancer values only
0
-20
-40
-60
-80
normal
cancer
liver
brain/glia
thyroid
connective tissue
epithelium

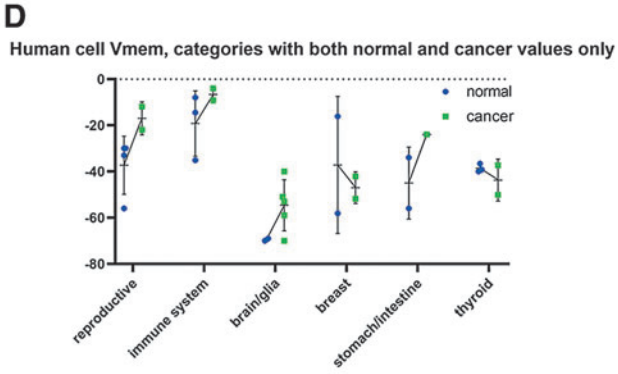
D
Human cell Vmem, categories with both normal and cancer values only
0
-20
-40
-60
-80
normal
cancer
reproductive
immune system
brain/glia
breast
stomach/intestine
thyroid

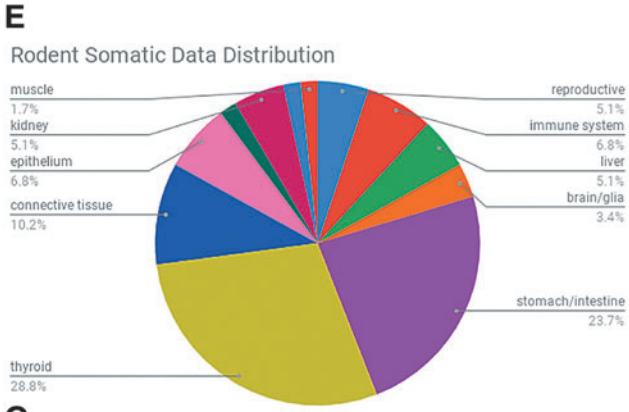
E
Rodent Somatic Data Distribution
muscle
1.7%
kidney
5.1%
epithelium
6.8%
connective tissue
10.2%
thyroid
28.8%
stomach/intestine
23.7%
brain/glia
3.4%
liver
5.1%
immune system
6.8%
reproductive
5.1%

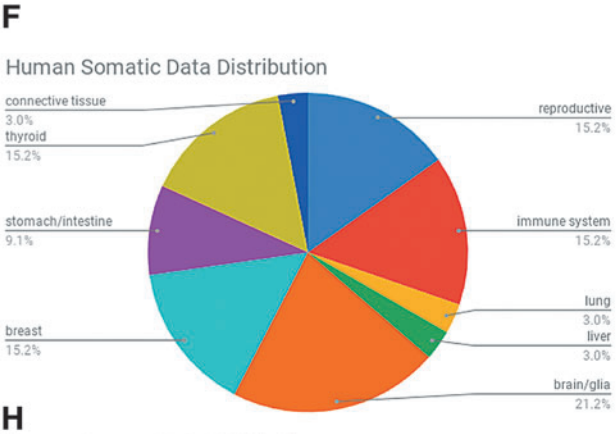
F
Human Somatic Data Distribution
connective tissue
3.0%
thyroid
15.2%
stomach/intestine
9.1%
breast
15.2%
brain/glia
21.2%
liver
3.0%
lung
3.0%
immune system
15.2%
reproductive
15.2%

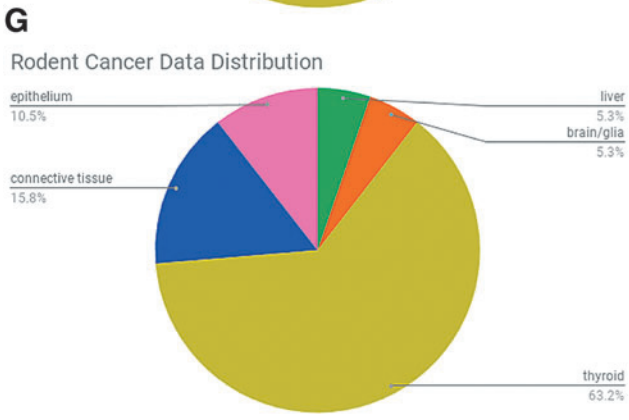
G
Rodent Cancer Data Distribution
epithelium
10.5%
connective tissue
15.8%
thyroid
63.2%
brain/glia
5.3%
liver
5.3%

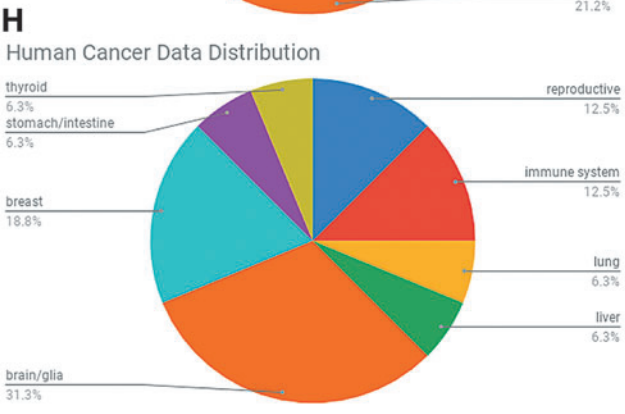
H
Human Cancer Data Distribution
thyroid
6.3%
stomach/intestine
6.3%
breast
18.8%
brain/glia
31.3%
liver
6.3%
lung
6.3%
immune system
12.5%
reproductive
12.5%

Table 7. Human Cell V_{mem} Measurements

	Average normal cell V_{mem}	*Average cancer cell V_{mem}*	*Cancer/normal cell V_{mem} ratio*	*Normal–cancer cell V_{mem} difference*
Reproductive	–31	–17	0.5	–14
Immune system	–19	–7	0.3	–12
Lung	NA	–33	NA	NA
Liver	NA	–7	NA	NA
Brain/glia	–70	–55	0.8	–15
Breast	–37	–36	1.0	–1
Stomach/intestine	–45	–24	0.5	–21
Thyroid	–38	–50	1.0	12

NA, not available.

somatic tissue versus cancer (human cancer-somatic delta = 16.0, 95% confidence interval [CI]: 1.1–30.8, $p = 0.0343$, rodent cancer-somatic delta = 32.3, 95% CI: 8.8–55.7, $p = 0.0068$), although significant heterogeneity between studies was observed in both human and rodent studies (Tables 7 and 8).

Furthermore, cancer cells seemed to fall within a narrower V_{mem} range than somatic cells such that the cancer cells derived from more hyperpolarized somatic cells showed a greater change in V_{mem} than those that were derived from less hyperpolarized cells (Fig. 3B, mixed-effects model $y = -16.9 - 0.85x$, where y is the difference between cancer and somatic V_{mem} and x is the somatic V_{mem}, $p < 0.0001$). While this relationship appears to be maintained when the cells are grouped by tissue type, we did not have a sufficient number of studies to determine whether this is a statistically significant relationship or not. The studies report that V_{mem} values in rodent cancer lines between −38 and −15 mV (a 23 mV difference) compared with a −96 to −30 mV variance in somatic tissues (a 66 mV difference) (Fig. 3C).

Interestingly, while the variance was broad, all rodent cancer cells had about half the V_{mem} of their corresponding somatic cells (Table 8), suggesting a linear relationship between somatic and cancerous cell V_{mem}. In human tissues, cancer cells may have a more depolarized V_{mem} (Fig. 3D), but insufficient published data are available to give significance. Regardless, the relationship between cancer and somatic cells was complicated, with some tissue types showing hyperpolarization in cancer (thyroid) (Fig. 3D) and more variation in the fold change over somatic V_{mem} (Table 7). While it is as yet unknown why thyroid cancer contradicts the general trend, such exceptions could be informative; for example, it may be due to the fact that most thyroid cancers are differentiated cancers, which may be expected to exhibit the more hyperpolarized values of differentiated cells. Overall, we find that a comprehensive analysis of V_{mem} measurements reveal a consistent hyperpolarized relationship between somatic tissue and cancer, with variation dependent on tissue type and model system.

Because this is a meta-analysis, we are limited by the types of V_{mem} characterization performed in the literature. Moreover, these values were determined by workers using diverse electrophysiological techniques, which may not be uniform across the dataset. Figure 2E–H shows the distribution of cell subtypes from which we were able to collect V_{mem} information. The rodent dataset lacks V_{mem} values for many cancer subtypes that have corresponding somatic tissue values and thyroid is over-represented, but otherwise the cell types cover a broad range of cancerous and somatic tissues. The values found for human somatic and cancerous tissues were distributed across many tissue types, and we found similar representation between somatic and cancerous tissue types, indicating that the data in human tissues might be the most reflective of general cancer versus somatic tissue phenotypes. It is clear however that comprehensive profiling of diverse cancer types, from multiple patients/cell lines in each

Table 8. Rodent Cell V_{mem} Measurements

	Average normal cell V_{mem}	*Average cancer cell V_{mem}*	*Cancer/normal cell V_{mem} ratio*	*Normal–cancer cell V_{mem} difference*
Reproductive	–43	NA	NA	NA
Immune system	–30	NA	NA	NA
Lung	NA	NA	NA	NA
Liver	–45	–20	0.4	–25
Brain/glia	–71	–38	0.5	–33
Breast	NA	NA	NA	NA
Stomach/intestine	–47	NA	NA	NA
Thyroid	–47	–26	0.5	–21
Connective tissue	–30	–20	0.6	–10
Epithelium	–30	–15	0.5	–15
Adipose tissue	–51	NA	NA	NA
Kidney	–56	NA	NA	NA
Pancreas	–41	NA	NA	NA
Muscle	–96	NA	NA	NA

category, using identical electrode types and extracellular media, will be an important component of future work.

Conclusion

Developmental bioelectricity is currently at a very exciting point, because physiology data are beginning to be integrated with molecular genetics. This is enabling a better understanding of the controls of growth and form at many scales, from single-cell behavior to multicell cooperation in organ morphogenesis.

The meta-analysis presented here uncovered some important patterns. First, a large number of channelopathies reveal the genetic basis for some bioelectric disorders. This list will certainly continue to grow as more model systems' genomes receive better coverage, but this will always be an underestimate because of the rich ability of physiological networks to drive complex dynamics even when the protein profile of cells is not altered. A comparison of phenotypes arising from genetic versus physiological stress will shed welcome light on the relationship between genome and anatomy. Many other genomic and profiling large datasets should be mined for interesting patterns of ion channel gene involvement.

Second, we reveal the remarkable fact that a small core of genes is strongly conserved with respect to expression in the regeneration blastema across Phyla. One target, the V-ATPase, which is conserved even across Kingdoms, is likely to be a critical part of repair. It was either harnessed at least twice by independent origins of multicellularity, or was already utilized by the unicellular ancestor for similar functions. This aspect, and the V-ATPase function in unicellular and multicellular morphogenesis, represents an important area for future research.

Finally, we report a higher resolution study of the bioelectric signature of cancer. The patterns we identified point to the urgent need for more data: many more normal and transformed cell types need to be profiled for their bioelectric state, to better understand the physiological controls of cellular cooperation in morphogenesis and defection by cancer cells. It is clear that physiomic profiling is a gap and opportunity for inclusion in genomic, transcriptomic, proteomic, and epigenetic global profiling efforts.

Because of its central role in neural function and embryogenesis, progress in bioelectricity has huge implications not only for basic understanding of evolution and developmental biology but also for regenerative medicine and synthetic bioengineering that impact numerous areas of the biosciences.

Author Contributions

P.S., A.K., C.H., and M.L. analyzed data, wrote text, and made figures. All coauthors have reviewed and approved the article before submission.

Author Disclosure Statement

The authors confirm there is no conflict of interest, actual or potential, for each listed author. No competing financial interests exist.

Funding Information

The authors gratefully acknowledge support of the Allen Discovery Center program through The Paul G. Allen Frontiers Group (12171) and the Barton Family Foundation.

Supplementary Material

Supplementary Table S1

References

1. Funk R. Ion gradients in tissue and organ biology. Biol Syst 2013;2:105.
2. Bates E. Ion channels in development and cancer. Annu Rev Cell Dev Biol 2015;31:231–247.
3. McLaughlin KA, Levin M. Bioelectric signaling in regeneration: Mechanisms of ionic controls of growth and form. Dev Biol 2018;433:177–189.
4. Levin M, Pezzulo G, Finkelstein JM. Endogenous bioelectric signaling networks: exploiting voltage gradients for control of growth and form. Annu Rev Biomed Eng 2017;19:353–387.
5. Mathews J, Levin M. Gap junctional signaling in pattern regulation: Physiological network connectivity instructs growth and form. Dev Neurobiol 2017;77: 643–673.
6. Funk RH. Endogenous electric fields as guiding cue for cell migration. Front Physiol 2015;6:143.
7. Zhao M. Electrical fields in wound healing—An overriding signal that directs cell migration. Semin Cell Dev Biol 2009;20:674–682.
8. George LF, Pradhan SJ, Mitchell D, et al. Ion channel contributions to wing development in *Drosophila melanogaster*. G3 (Bethesda) 2019;9:999–1008.
9. Pai VP, Lemire JM, Pare JF, et al. Endogenous gradients of resting potential instructively pattern embryonic neural tissue via notch signaling and regulation of proliferation. J Neurosci 2015;35:4366–4385.
10. Adams DS, Uzel SG, Akagi J, et al. Bioelectric signalling via potassium channels: A mechanism for craniofacial dysmorphogenesis in KCNJ2-associated Andersen-Tawil Syndrome. J Physiol 2016;594:3245–3270.
11. Durant F, Morokuma J, Fields C, et al. Long-term, stochastic editing of regenerative anatomy via targeting endogenous bioelectric gradients. Biophys J 2017;112:2231–2243.
12. Perathoner S, Daane JM, Henrion U, et al. Bioelectric signaling regulates size in zebrafish fins. PLoS Genet 2014;10:e1004080.
13. Levin M, Martyniuk CJ. The bioelectric code: An ancient computational medium for dynamic control of growth and form. Biosystems 2018;164:76–93.
14. Levin M. Morphogenetic fields in embryogenesis, regeneration, and cancer: Non-local control of complex patterning. Biosystems 2012;109:243–261.
15. Mathews J, Levin M. The body electric 2.0: Recent advances in developmental bioelectricity for regenerative and synthetic bioengineering. Curr Opin Biotechnol 2018; 52:134–144.
16. Hernandez-Diaz S, Levin M. Alteration of bioelectrically-controlled processes in the embryo: A teratogenic mechanism for anticonvulsants. Reprod Toxicol 2014;47:111–114.
17. Levin M. The wisdom of the body: Future techniques and approaches to morphogenetic fields in regenerative medicine, developmental biology and cancer. Regen Med 2011;6:667–673.
18. Reid B, Zhao M. The electrical response to injury: Molecular mechanisms and wound healing. Adv Wound Care (New Rochelle) 2014;3:184–201.

19. Bates EA. A potential molecular target for morphological defects of fetal alcohol syndrome: Kir2.1. Curr Opin Genet Dev 2013;23:324–329.
20. Dahal GR, Pradhan SJ, Bates EA. Inwardly rectifying potassium channels influence Drosophila wing morphogenesis by regulating Dpp release. Development 2017; 144:2771–2783.
21. Pitcairn E, Harris H, Epiney J, et al. Coordinating heart morphogenesis: A novel role for Hyperpolarization-activated cyclic nucleotide-gated (HCN) channels during cardiogenesis in Xenopus laevis. Commun Integr Biol 2017;10:e1309488.
22. Levin M, Thorlin T, Robinson KR, et al. Asymmetries in H+/K+-ATPase and cell membrane potentials comprise a very early step in left-right patterning. Cell 2002;111: 77–89.
23. Moore D, Walker SI, Levin M. Cancer as a disorder of patterning information: Computational and biophysical perspectives on the cancer problem. Converg Sci Phys Oncol 2017;3:043001.
24. Rubin H. Cancer as a dynamic developmental disorder. Cancer Res 1985;45:2935–2942.
25. Sonnenschein C, Soto AM. The Society of Cells: Cancer Control of Cell Proliferation. Oxford, New York: Springer, 1999: xiv, 154.
26. Burr HS. Biologic organization and the cancer problem. Yale J Biol Med 1940;12:277–282.
27. Cone CD, Tongier M. Control of somatic cell mitosis by simulated changes in the transmembrane potential level. Oncology 1971;25:168–182.
28. Cone CD. Unified theory on the basic mechanism of normal mitotic control and oncogenesis. J Theor Biol 1971;30:151–181.
29. Lobikin M, Chernet B, Lobo D, et al. Resting potential, oncogene-induced tumorigenesis, and metastasis: The bioelectric basis of cancer in vivo. Phys Biol 2012;9:065002.
30. Djamgoz MB, Coombes RC, Schwab A. Ion transport and cancer: From initiation to metastasis. Philos Trans R Soc Lond B Biol Sci 2014;369:20130092.
31. Chernet BT, Adams DS, Lobikin M, et al. Use of genetically encoded, light-gated ion translocators to control tumorigenesis. Oncotarget 2016;7:19575–19588.
32. Gentile S. hERG1 potassium channel in cancer cells: A tool to reprogram immortality. Eur Biophys J 2016;45:649–655.
33. Birnbaum KD, Alvarado AS. Slicing across kingdoms: Regeneration in plants and animals. Cell 2008;132:697–710.
34. Maden M. The evolution of regeneration—Where does that leave mammals? Int J Dev Biol 2018;62:369–372.
35. Larkin JW, Zhai X, Kikuchi K, et al. Signal percolation within a bacterial community. Cell Syst 2018;7:137–145.e3.
36. Liu J, Martinez-Corral R, Prindle A, et al. Coupling between distant biofilms and emergence of nutrient time-sharing. Science 2017;356:638–642.
37. Prindle A, Liu J, Asally M, et al. Ion channels enable electrical communication in bacterial communities. Nature 2015;527:59–63.
38. Levin M, Selberg J, Rolandi M. Endogenous bioelectrics in development, cancer, and regeneration: Drugs and bioelectronic devices as electroceuticals for regenerative medicine. iScience 2019;22:519–533.
39. Whited JL, Levin M. Bioelectrical controls of morphogenesis: From ancient mechanisms of cell coordination to biomedical opportunities. Curr Opin Genet Dev 2019;57: 61–69.
40. Marino AA, Iliev IG, Schwalke MA, et al. Association between cell membrane potential and breast cancer. Tumour Biol 1994;15:82–89.
41. Binggeli R, Weinstein RC. Deficits in elevating membrane potential of rat fibrosarcoma cells after cell contact. Cancer Res 1985;45:235–241.
42. Pereda AE, Curti S, Hoge G, et al. Gap junction-mediated electrical transmission: Regulatory mechanisms and plasticity. Biochim Biophys Acta 2013;1828:134–146.
43. Palacios-Prado N, Bukauskas FF. Heterotypic gap junction channels as voltage-sensitive valves for intercellular signaling. Proc Natl Acad Sci U S A 2009;106:14855–14860.
44. Manicka S, Levin M. Modeling somatic computation with non-neural bioelectric networks. Sci Rep 2019;9:18612.
45. Bult CJ, Blake JA, Smith CL, et al. Mouse Genome Database (MGD) 2019. Nucleic Acids Res 2019;47:D801–D806.
46. Howe DG, Bradford YM, Conlin T, et al. ZFIN, the Zebrafish Model Organism Database: Increased support for mutants and transgenics. Nucleic Acids Res 2013;41: D854–D860.
47. Thurmond J, Goodman JL, Strelets VB, et al. FlyBase 2.0: The next generation. Nucleic Acids Res 2019;47:D759–D765.
48. Mummery-Widmer JL, Yamazaki M, Stoeger T, et al. Genome-wide analysis of Notch signalling in Drosophila by transgenic RNAi. Nature 2009;458:987–992.
49. Wu CH, Tsai MH, Ho CC, et al. De novo transcriptome sequencing of axolotl blastema for identification of differentially expressed genes during limb regeneration. BMC Genomics 2013;14:434.
50. Kao D, Felix D, Aboobaker A. The planarian regeneration transcriptome reveals a shared but temporally shifted regulatory program between opposing head and tail scenarios. BMC Genomics 2013;14:797.
51. Leinonen R, Sugawara H, Shumway M, et al. The sequence read archive. Nucleic Acids Res 2011;39:D19–D21.
52. Barrett T, Wilhite SE, Ledoux P, et al. NCBI GEO: Archive for functional genomics data sets—Update. Nucleic Acids Res 2013;41:D991–D995.
53. Huerta-Cepas J, Forslund K, Coelho LP, et al. Fast genome-wide functional annotation through orthology assignment by eggNOG-Mapper. Mol Biol Evol 2017;34: 2115–2122.
54. Huerta-Cepas J, Szklarczyk D, Forslund K, et al. eggNOG 4.5: A hierarchical orthology framework with improved functional annotations for eukaryotic, prokaryotic and viral sequences. Nucleic Acids Res 2016;44:D286–D293.
55. Liberzon A, Birger C, Thorvaldsdottir H, et al. The Molecular Signatures Database (MSigDB) hallmark gene set collection. Cell Syst 2015;1:417–425.
56. Khare S, Nick JA, Zhang Y, et al. A KCNC3 mutation causes a neurodevelopmental, non-progressive SCA13 subtype associated with dominant negative effects and aberrant EGFR trafficking. PLoS One 2017;12:e0173565.
57. Pai VP, Aw S, Shomrat T, et al. Transmembrane voltage potential controls embryonic eye patterning in Xenopus laevis. Development 2012;139:313–323.
58. Adams DS, Masi A, Levin M. H+ pump-dependent changes in membrane voltage are an early mechanism necessary and sufficient to induce Xenopus tail regeneration. Development 2007;134:1323–1335.

59. Tseng AS, Beane WS, Lemire JM, et al. Induction of vertebrate regeneration by a transient sodium current. J Neurosci 2010;30:13192–13200.
60. Chernet BT, Fields C, Levin M. Long-range gap junctional signaling controls oncogene-mediated tumorigenesis in Xenopus laevis embryos. Front Physiol 2015;5:519.
61. Chernet BT, Levin M. Transmembrane voltage potential of somatic cells controls oncogene-mediated tumorigenesis at long-range. Oncotarget 2014;5:3287–3306.
62. Chernet BT, Levin M. Transmembrane voltage potential is an essential cellular parameter for the detection and control of tumor development in a Xenopus model. Dis Model Mech 2013;6:595–607.
63. Bonnet S, Archer SL, Allalunis-Turner J, et al. A mitochondria-K+ channel axis is suppressed in cancer and its normalization promotes apoptosis and inhibits cancer growth. Cancer Cell 2007;11:37–51.
64. Gomez-Varela D, Zwick-Wallasch E, Knotgen H, et al. Monoclonal antibody blockade of the human Eag1 potassium channel function exerts antitumor activity. Cancer Res 2007;67:7343–7349.
65. Isbilen B, Fraser SP, Djamgoz MB. Docosahexaenoic acid (omega-3) blocks voltage-gated sodium channel activity and migration of MDA-MB-231 human breast cancer cells. Int J Biochem Cell Biol 2006;38:2173–2182.
66. Ohkubo T, Yamazaki J. T-type voltage-activated calcium channel Cav3.1, but not Cav3.2, is involved in the inhibition of proliferation and apoptosis in MCF-7 human breast cancer cells. Int J Oncol 2012;41:267–275.
67. Wang H, Zhang Y, Cao L, et al. HERG K+ channel, a regulator of tumor cell apoptosis and proliferation. Cancer Res 2002;62:4843–4848.
68. Warnier M, Roudbaraki M, Derouiche S, et al. CACNA2D2 promotes tumorigenesis by stimulating cell proliferation and angiogenesis. Oncogene 2015;34:5383–5394.
69. Beane WS, Morokuma J, Adams DS, et al. A Chemical genetics approach reveals H,K-ATPase-mediated membrane voltage is required for planarian head regeneration. Chem Biol 2011;18:77–89.
70. Vandenberg LN, Morrie RD, Adams DS. V-ATPase-dependent ectodermal voltage and pH regionalization are required for craniofacial morphogenesis. Dev Dyn 2011; 240:1889–1904.
71. Yemini E, Jucikas T, Grundy LJ, et al. A database of *Caenorhabditis elegans* behavioral phenotypes. Nat Methods 2013;10:877–879.
72. Koni PA, Khanna R, Chang MC, et al. Compensatory anion currents in Kv1.3 channel-deficient thymocytes. J Biol Chem 2003;278:39443–39451.
73. Kim EZ, Vienne J, Rosbash M, et al. Non-reciprocal homeostatic compensation in Drosophila potassium channel mutants. J Neurophysiol 2017;117:2125–2136.
74. Levin M. Isolation and community: A review of the role of gap-junctional communication in embryonic patterning. J Membr Biol 2002;185:177–192.
75. Gokey JJ, Dasgupta A, Amack JD. The V-ATPase accessory protein Atp6ap1b mediates dorsal forerunner cell proliferation and left-right asymmetry in zebrafish. Dev Biol 2015;407:115–130.
76. Adams DS, Robinson KR, Fukumoto T, et al. Early, H+-V-ATPase-dependent proton flux is necessary for consistent left-right patterning of non-mammalian vertebrates. Development 2006;133:1657–1671.
77. Nuckels RJ, Ng A, Darland T, et al. The vacuolar-ATPase complex regulates retinoblast proliferation and survival, photoreceptor morphogenesis, and pigmentation in the zebrafish eye. Invest Ophthalmol Vis Sci 2009;50: 893–905.
78. Fraire-Zamora JJ, Simons M. The vacuolar ATPase is required for ERK-dependent wound healing in the Drosophila embryo. Wound Repair Regen 2018;26:102–107.
79. Lange C, Prenninger S, Knuckles P, et al. The H(+) vacuolar ATPase maintains neural stem cells in the developing mouse cortex. Stem Cells Dev 2011;20:843–850.
80. Harvey WR, Wieczorek H. Animal plasma membrane energization by chemiosmotic H+ V-ATPases. J Exp Biol 1997;200 (Pt 2):203–216.
81. Hinton A, Bond S, Forgac M. V-ATPase functions in normal and disease processes. Pflugers Arch 2009;457: 589–598.
82. Finbow ME, Harrison M, Jones P. Ductin—A proton pump component, a gap junction channel and a neurotransmitter release channel. Bioessays 1995;17:247–255.
83. Dunlop J, Jones PC, Finbow ME. Membrane insertion and assembly of ductin: A polytopic channel with dual orientations. EMBO J 1995;14:3609–3616.
84. Bruzzone R, Goodenough DA. Gap junctions: Ductin or connexins—Which component is the critical one? Bioessays 1995;17:744–745.
85. Finbow ME, Goodwin SF, Meagher L, et al. Evidence that the 16 kDa proteolipid (subunit c) of the vacuolar H(+)-ATPase and ductin from gap junctions are the same polypeptide in Drosophila and Manduca: Molecular cloning of the Vha16k gene from Drosophila. J Cell Sci 1994;107 (Pt 7):1817–1824.
86. Finbow ME, Pitts JD. Is the gap junction channel—The connexon—Made of connexin or ductin? J Cell Sci 1993; 106:463–471.
87. Cone CD, Cone CM. Induction of mitosis in mature neurons in central nervous system by sustained depolarization. Science 1976;192:155–158.
88. Cone CD. The role of the surface electrical transmembrane potential in normal and malignant mitogenesis. Ann NY Acad Sci 1974;238:420–435.
89. Borthwick KJ, Kandemir N, Topaloglu R, et al. A phenocopy of CAII deficiency: A novel genetic explanation for inherited infantile osteopetrosis with distal renal tubular acidosis. J Med Genet 2003;40:115–121.
90. Tamirisa S, Papagiannouli F, Rempel E, et al. Decoding the regulatory logic of the Drosophila male stem cell system. Cell Rep 2018;24:3072–3086.
91. Masotti A, Uva P, Davis-Keppen L, et al. Keppen-Lubinsky syndrome is caused by mutations in the inwardly rectifying K(+) channel encoded by KCNJ6. Am J Hum Genet 2015; 96:295–300.
92. Kortum F, Caputo V, Bauer CK, et al. Mutations in KCNH1 and ATP6V1B2 cause Zimmermann-Laband syndrome. Nat Genet 2015;47:661–667.
93. Simons C, Rash LD, Crawford J, et al. Mutations in the voltage-gated potassium channel gene KCNH1 cause Temple-Baraitser syndrome and epilepsy. Nat Genet 2015;47:73–77.
94. Labonne JD, Graves TD, Shen Y, et al. A microdeletion at Xq22.2 implicates a glycine receptor GLRA4 involved in intellectual disability, behavioral problems and craniofacial anomalies. BMC Neurol 2016;16:132.

95. Hiraki Y, Miyatake S, Hayashidani M, et al. Aortic aneurysm and craniosynostosis in a family with Cantu syndrome. Am J Med Genet A 2014;164A:231–236.
96. Cooper PE, Reutter H, Woelfle J, et al. Cantu syndrome resulting from activating mutation in the KCNJ8 gene. Hum Mutat 2014;35:809–813.
97. Brownstein CA, Towne MC, Luquette LJ, et al. Mutation of KCNJ8 in a patient with Cantu syndrome with unique vascular abnormalities—Support for the role of K(ATP) channels in this condition. Eur J Med Genet 2013;56:678–682.
98. Chong JX, McMillin MJ, Shively KM, et al. De novo mutations in NALCN cause a syndrome characterized by congenital contractures of the limbs and face, hypotonia, and developmental delay. Am J Hum Genet 2015;96:462–473.
99. Uzun S, Gokce S, Wagner K. Cystic fibrosis transmembrane conductance regulator gene mutations in infertile males with congenital bilateral absence of the vas deferens. Tohoku J Exp Med 2005;207:279–285.
100. Wilschanski M, Dupuis A, Ellis L, et al. Mutations in the cystic fibrosis transmembrane regulator gene and in vivo transepithelial potentials. Am J Respir Crit Care Med 2006;174:787–794.
101. Smith RS, Kenny CJ, Ganesh V, et al. Sodium channel SCN3A (NaV1.3) regulation of human cerebral cortical folding and oral motor development. Neuron 2018;99:905–913.e907.
102. Hutson MR, Keyte AL, Hernandez-Morales M, et al. Temperature-activated ion channels in neural crest cells confer maternal fever-associated birth defects. Sci Signal 2017;10:pii: eaal4055.
103. Poirier K, Viot G, Lombardi L, et al. Loss of Function of KCNC1 is associated with intellectual disability without seizures. Eur J Hum Genet 2017;25:560–564.
104. Veale EL, Hassan M, Walsh Y, et al. Recovery of current through mutated TASK3 potassium channels underlying Birk Barel syndrome. Mol Pharmacol 2014;85:397–407.
105. Barel O, Shalev SA, Ofir R, et al. Maternally inherited Birk Barel mental retardation dysmorphism syndrome caused by a mutation in the genomically imprinted potassium channel KCNK9. Am J Hum Genet 2008;83:193–199.
106. Bando Y, Hirano T, Tagawa Y. Dysfunction of KCNK potassium channels impairs neuronal migration in the developing mouse cerebral cortex. Cereb Cortex 2014;24:1017–1029.
107. Gloyn AL, Pearson ER, Antcliff JF, et al. Activating mutations in the gene encoding the ATP-sensitive potassium-channel subunit Kir6.2 and permanent neonatal diabetes. N Eng J Med 2004;350:1838–1849.
108. Lee MP, Ravenel JD, Hu RJ, et al. Targeted disruption of the Kvlqt1 gene causes deafness and gastric hyperplasia in mice. J Clin Invest 2000;106:1447–1455.
109. Weksberg R, Nishikawa J, Caluseriu O, et al. Tumor development in the Beckwith-Wiedemann syndrome is associated with a variety of constitutional molecular 11p15 alterations including imprinting defects of KCNQ1OT1. Hum Mol Genet 2001;10:2989–3000.
110. Moore ES, Ward RE, Escobar LF, et al. Heterogeneity in Wiedemann-Beckwith syndrome: Anthropometric evidence. Am J Med Genet 2000;90:283–290.
111. Wen H, Weiger TM, Ferguson TS, et al. A Drosophila KCNQ channel essential for early embryonic development. J Neurosci 2005;25:10147–10156.
112. Rivas A, Francis HW. Inner ear abnormalities in a Kcnq1 (Kvlqt1) knockout mouse: A model of Jervell and Lange-Nielsen syndrome. Otol Neurotol 2005;26:415–424.
113. Casimiro MC, Knollmann BC, Yamoah EN, et al. Targeted point mutagenesis of mouse Kcnq1: Phenotypic analysis of mice with point mutations that cause Romano-Ward syndrome in humans. Genomics 2004;84:555–564.
114. Chouabe C, Neyroud N, Guicheney P, et al. Properties of KvLQT1 K+ channel mutations in Romano-Ward and Jervell and Lange-Nielsen inherited cardiac arrhythmias. EMBO J 1997;16:5472–5479.
115. Bendahhou S, Donaldson MR, Plaster NM, et al. Defective potassium channel Kir2.1 trafficking underlies Andersen-Tawil syndrome. J Biol Chem 2003;278:51779–51785.
116. Dahal GR, Rawson J, Gassaway B, et al. An inwardly rectifying K+ channel is required for patterning. Development 2012;139:3653–3664.
117. Yoon G, Oberoi S, Tristani-Firouzi M, et al. Andersen-Tawil syndrome: Prospective cohort analysis and expansion of the phenotype. Am J Med Genet A 2006;140:312–321.
118. Fakhro KA, Choi M, Ware SM, et al. Rare copy number variations in congenital heart disease patients identify unique genes in left-right patterning. Proc Natl Acad Sci U S A 2011;108:2915–2920.
119. Splawski I, Timothy KW, Sharpe LM, et al. Ca(V)1.2 calcium channel dysfunction causes a multisystem disorder including arrhythmia and autism. Cell 2004;119:19–31.
120. Britz-Cunningham SH, Shah MM, Zuppan CW, et al. Mutations of the Connexin43 gap-junction gene in patients with heart malformations and defects of laterality. N Engl J Med 1995;332:1323–1329.
121. Debeer P, Van Esch H, Huysmans C, et al. Novel GJA1 mutations in patients with oculo-dento-digital dysplasia (ODDD). Eur J Med Genet 2005;48:377–387.
122. Pizzuti A, Flex E, Mingarelli R, et al. A homozygous GJA1 gene mutation causes a Hallermann-Streiff/ODDD spectrum phenotype. Hum Mutat 2004;23:286.
123. Villanueva S, Burgos J, Lopez-Cayuqueo KI, et al. Cleft palate, moderate lung developmental retardation and early postnatal lethality in mice deficient in the Kir7.1 inwardly rectifying K+ channel. PLoS One 2015;10:e0139284.
124. Zheng J, Trudeau MC. Handbook of Ion Channels. Boca Raton, FL: CRC Press, 2015; xx, 671.
125. Duque A, Gazula VR, Kaczmarek LK. Expression of Kv1.3 potassium channels regulates density of cortical interneurons. Dev Neurobiol 2013;73:841–855.
126. Stobrawa SM, Breiderhoff T, Takamori S, et al. Disruption of ClC-3, a chloride channel expressed on synaptic vesicles, leads to a loss of the hippocampus. Neuron 2001;29:185–196.
127. Christensen AH, Chatelain FC, Huttner IG, et al. The two-pore domain potassium channel, TWIK-1, has a role in the regulation of heart rate and atrial size. J Mol Cell Cardiol 2016;97:24–35.
128. Petersson S, Persson AS, Johansen JE, et al. Truncation of the Shaker-like voltage-gated potassium channel, Kv1.1, causes megencephaly. Eur J Neurosci 2003;18:3231–3240.
129. Zhou Y, Zhu J, Lv Y, et al. Kir6.2 deficiency promotes mesencephalic neural precursor cell differentiation via regulating miR-133b/GDNF in a Parkinson's disease mouse model. Mol Neurobiol 2018;55:8550–8562.

130. Takagi T, Nishio H, Yagi T, et al. Phenotypic analysis of vertigo 2 Jackson mice with a Kcnq1 potassium channel mutation. Exp Anim 2007;56:295–300.
131. Than BL, Goos JA, Sarver AL, et al. The role of KCNQ1 in mouse and human gastrointestinal cancers. Oncogene 2014;33:3861–3868.
132. Belus MT, Rogers MA, Elzubeir A, et al. Kir2.1 is important for efficient BMP signaling in mammalian face development. Dev Biol 2018;444 Suppl 1:S297–S307.
133. Culiat CT, Stubbs LJ, Woychik RP, et al. Deficiency of the beta 3 subunit of the type A gamma-aminobutyric acid receptor causes cleft palate in mice. Nat Genet 1995;11: 344–346.
134. Wee EL, Zimmerman EF. GABA uptake in embryonic palate mesenchymal cells of two mouse strains. Neurochem Res 1985;10:1673–1688.
135. Homanics GE, DeLorey TM, Firestone LL, et al. Mice devoid of gamma-aminobutyrate type A receptor beta3 subunit have epilepsy, cleft palate, and hypersensitive behavior. Proc Natl Acad Sci U S A 1997;94:4143–4148.
136. Maison SF, Rosahl TW, Homanics GE, et al. Functional role of GABAergic innervation of the cochlea: Phenotypic analysis of mice lacking GABA(A) receptor subunits alpha 1, alpha 2, alpha 5, alpha 6, beta 2, beta 3, or delta. J Neurosci 2006;26:10315–10326.
137. DeLorey TM, Sahbaie P, Hashemi E, et al. Gabrb3 gene deficient mice exhibit impaired social and exploratory behaviors, deficits in non-selective attention and hypoplasia of cerebellar vermal lobules: A potential model of autism spectrum disorder. Behav Brain Res 2008;187:207–220.
138. Rock JR, Futtner CR, Harfe BD. The transmembrane protein TMEM16A is required for normal development of the murine trachea. Dev Biol 2008;321:141–149.
139. Rakic P, Sidman RL. Sequence of developmental abnormalities leading to granule cell deficit in cerebellar cortex of weaver mutant mice. J Comp Neurol 1973;152:103–132.
140. Rakic P, Sidman RL. Weaver mutant mouse cerebellum: Defective neuronal migration secondary to abnormality of Bergmann glia. Proc Natl Acad Sci U S A 1973;70:240–244.
141. Hatten ME, Liem RK, Mason CA. Weaver mouse cerebellar granule neurons fail to migrate on wild-type astroglial processes in vitro. J Neurosci Nurs 1986;6:2676–2683.
142. Patil N, Cox DR, Bhat D, et al. A potassium channel mutation in weaver mice implicates membrane excitability in granule cell differentiation. Nat Genet 1995;11:126–129.
143. Teng GQ, Zhao X, Lees-Miller JP, et al. Homozygous missense N629D hERG (KCNH2) potassium channel mutation causes developmental defects in the right ventricle and its outflow tract and embryonic lethality. Circ Res 2008;103:1483–1491.
144. Tur J, Chapalamadugu KC, Padawer T, et al. Deletion of Kvbeta1.1 subunit leads to electrical and haemodynamic changes causing cardiac hypertrophy in female murine hearts. Exp Physiol 2016;101:494–508.
145. Dickinson ME, Flenniken AM, Ji X, et al. High-throughput discovery of novel developmental phenotypes. Nature 2016;537:508–514.
146. Blanz J, Schweizer M, Auberson M, et al. Leukoencephalopathy upon disruption of the chloride channel ClC-2. J Neurosci 2007;27:6581–6589.
147. Wang SS, Devuyst O, Courtoy PJ, et al. Mice lacking renal chloride channel, CLC-5, are a model for Dent's disease, a nephrolithiasis disorder associated with defective receptor-mediated endocytosis. Hum Mol Genet 2000;9:2937–2945.
148. Koval LM, Zverkova AS, Grailhe R, et al. Nicotinic acetylcholine receptors alpha4beta2 and alpha7 regulate myelo- and erythropoiesis within the bone marrow. Int J Biochem Cell Biol 2008;40:980–990.
149. Lin H, Hsu FC, Baumann BH, et al. Cortical parvalbumin GABAergic deficits with alpha7 nicotinic acetylcholine receptor deletion: Implications for schizophrenia. Mol Cell Neurosci 2014;61:163–175.
150. Mallon AM, Iyer V, Melvin D, et al. Accessing data from the International Mouse Phenotyping Consortium: State of the art and future plans. Mamm Genome 2012;23:641–652.
151. Takahashi M, Kubo T, Mizoguchi A, et al. Spontaneous muscle action potentials fail to develop without fetal-type acetylcholine receptors. EMBO Rep 2002;3:674–681.
152. Chang B, Wang X, Hawes NL, et al. A Gja8 (Cx50) point mutation causes an alteration of alpha 3 connexin (Cx46) in semi-dominant cataracts of Lop10 mice. Hum Mol Genet 2002;11:507–513.
153. White TW. Unique and redundant connexin contributions to lens development. Science 2002;295:319–320.
154. Frank M, Eiberger B, Janssen-Bienhold U, et al. Neuronal connexin-36 can functionally replace connexin-45 in mouse retina but not in the developing heart. J Cell Sci 2010;123:3605–3615.
155. Kumai M, Nishii K, Nakamura K, et al. Loss of connexin45 causes a cushion defect in early cardiogenesis. Development 2000;127:3501–3512.
156. Nishii K, Kumai M, Egashira K, et al. Mice lacking connexin45 conditionally in cardiac myocytes display embryonic lethality similar to that of germline knockout mice without endocardial cushion defect. Cell Commun Adhes 2003;10:365–369.
157. Nishii K, Kumai M, Shibata Y. Regulation of the epithelial-mesenchymal transformation through gap junction channels in heart development. Trends Cardiovasc Med 2001;11:213–218.
158. Araya R, Eckardt D, Riquelme MA, et al. Presence and importance of connexin43 during myogenesis. Cell Commun Adhes 2003;10:451–456.
159. Civitelli R. Cell-cell communication in the osteoblast/osteocyte lineage. Arch Biochem Biophys 2008;473:188–192.
160. Dobrowolski R, Hertig G, Lechner H, et al. Loss of connexin43-mediated gap junctional coupling in the mesenchyme of limb buds leads to altered expression of morphogens in mice. Hum Mol Genet 2009;18:2899–2911.
161. Ewart JL, Cohen MF, Meyer RA, et al. Heart and neural tube defects in transgenic mice overexpressing the Cx43 gap junction gene. Development 1997;124:1281–1292.
162. Lecanda F, Warlow PM, Sheikh S, et al. Connexin43 deficiency causes delayed ossification, craniofacial abnormalities, and osteoblast dysfunction. J Cell Biol 2000; 151:931–944.
163. Reaume AG, de Sousa PA, Kulkarni S, et al. Cardiac malformation in neonatal mice lacking connexin43. Science 1995;267:1831–1834.
164. Davy A, Bush JO, Soriano P. Inhibition of gap junction communication at ectopic Eph/ephrin boundaries underlies craniofrontonasal syndrome. PLoS Biol 2006;4:e315.

165. Kanady JD, Dellinger MT, Munger SJ, et al. Connexin37 and Connexin43 deficiencies in mice disrupt lymphatic valve development and result in lymphatic disorders including lymphedema and chylothorax. Dev Biol 2011; 354:253–266.
166. Kanady JD, Munger SJ, Witte MH, et al. Combining Foxc2 and Connexin37 deletions in mice leads to severe defects in lymphatic vascular growth and remodeling. Dev Biol 2015;405:33–46.
167. Chang Q, Tang W, Kim Y, et al. Timed conditional null of connexin26 in mice reveals temporary requirements of connexin26 in key cochlear developmental events before the onset of hearing. Neurobiol Dis 2015;73:418–427.
168. Pizard A, Burgon PG, Paul DL, et al. Connexin 40, a target of transcription factor tbx5, patterns wrist, digits, and sternum. Mol Cell Biol 2005;25:5073–5083.
169. Oh SK, Shin JO, Baek JI, et al. Pannexin 3 is required for normal progression of skeletal development in vertebrates. FASEB J 2015;29:4473–4484.
170. Meier H, Chai CK. Spastic, an hereditary neurological mutation in the mouse characterized by vertebral arthropathy and leptomeningeal cyst formation. Exp Med Surg 1970;28:24–38.
171. Yin W, Kim HT, Wang S, et al. The potassium channel KCNJ13 is essential for smooth muscle cytoskeletal organization during mouse tracheal tubulogenesis. Nat Commun 2018;9:2815.
172. Pradervand S, Wang Q, Burnier M, et al. A mouse model for Liddle's syndrome. J Am Soc Nephrol 1999;10:2527–2533.
173. Bett GC, Lis A, Wersinger SR, et al. A mouse model of Timothy syndrome: A complex autistic disorder resulting from a point mutation in Cav1.2. N Am J Med Sci (Boston) 2012;5:135–140.
174. Fu Y, Westenbroek RE, Yu FH, et al. Deletion of the distal C terminus of CaV1.2 channels leads to loss of beta-adrenergic regulation and heart failure in vivo. J Biol Chem 2011;286:12617–12626.
175. Patel N, Smith LL, Faqeih E, et al. ZBTB42 mutation defines a novel lethal congenital contracture syndrome (LCCS6). Hum Mol Genet 2014;23:6584–6593.
176. Chopra SS, Stroud DM, Watanabe H, et al. Voltage-gated sodium channels are required for heart development in zebrafish. Circ Res 2010;106:1342–1350.
177. Shu X, Cheng K, Patel N, et al. Na,K-ATPase is essential for embryonic heart development in the zebrafish. Development 2003;130:6165–6173.
178. Li IC, Chen YC, Wang YY, et al. Zebrafish Adar2 Edits the Q/R site of AMPA receptor Subunit gria2alpha transcript to ensure normal development of nervous system and cranial neural crest cells. PLoS One 2014;9:e97133.
179. Doganli C, Kjaer-Sorensen K, Knoeckel C, et al. The alpha2Na+/K+-ATPase is critical for skeletal and heart muscle function in zebrafish. J Cell Sci 2012;125:6166–6175.
180. Shu X, Huang J, Dong Y, et al. Na,K-ATPase alpha2 and Ncx4a regulate zebrafish left-right patterning. Development 2007;134:1921–1930.
181. Lamason RL, Mohideen MA, Mest JR, et al. SLC24A5, a putative cation exchanger, affects pigmentation in zebrafish and humans. Science 2005;310:1782–1786.
182. Liu F, Xia W, Hu J, et al. Solute carrier family 26 member a2 (slc26a2) regulates otic development and hair cell survival in zebrafish. PLoS One 2015;10:e0136832.
183. Prudent J, Popgeorgiev N, Bonneau B, et al. Bcl-wav and the mitochondrial calcium uniporter drive gastrula morphogenesis in zebrafish. Nat Commun 2013;4:2330.
184. Chernyavskaya Y, Ebert AM, Milligan E, et al. Voltage-gated calcium channel CACNB2 (beta2.1) protein is required in the heart for control of cell proliferation and heart tube integrity. Dev Dyn 2012;241:648–662.
185. Kucenas S, Cox JA, Soto F, et al. Ectodermal P2X receptor function plays a pivotal role in craniofacial development of the zebrafish. Purinergic Signal 2009;5:395–407.
186. Delcourt N, Quevedo C, Nonne C, et al. Targeted identification of sialoglycoproteins in hypoxic endothelial cells and validation in zebrafish reveal roles for proteins in angiogenesis. J Biol Chem 2015;290:3405–3417.
187. Faucherre A, Kissa K, Nargeot J, et al. Piezo1 plays a role in erythrocyte volume homeostasis. Haematologica 2014; 99:70–75.
188. Ebert AM, Hume GL, Warren KS, et al. Calcium extrusion is critical for cardiac morphogenesis and rhythm in embryonic zebrafish hearts. Proc Natl Acad Sci U S A 2005;102:17705–17710.
189. Shimizu H, Langenbacher AD, Huang J, et al. The Calcineurin-FoxO-MuRF1 signaling pathway regulates myofibril integrity in cardiomyocytes. Elife 2017;6:pii: e27955.
190. Choksi SP, Babu D, Lau D, et al. Systematic discovery of novel ciliary genes through functional genomics in the zebrafish. Development 2014;141:3410–3419.
191. Liang B, Soka M, Christensen AH, et al. Genetic variation in the two-pore domain potassium channel, TASK-1, may contribute to an atrial substrate for arrhythmogenesis. J Mol Cell Cardiol 2014;67:69–76.
192. Shim H, Kim JH, Kim CY, et al. Function-driven discovery of disease genes in zebrafish using an integrated genomics big data resource. Nucleic Acids Res 2016;44: 9611–9623.
193. Shen H, Bocksteins E, Kondrychyn I, et al. Functional antagonism of voltage-gated K+ channel alpha-subunits in the developing brain ventricular system. Development 2016;143:4249–4260.
194. Mahmood F, Mozere M, Zdebik AA, et al. Generation and validation of a zebrafish model of EAST (epilepsy, ataxia, sensorineural deafness and tubulopathy) syndrome. Dis Model Mech 2013;6:652–660.
195. Andersen ND, Ramachandran KV, Bao MM, et al. Calcium signaling regulates ventricular hypertrophy during development independent of contraction or blood flow. J Mol Cell Cardiol 2015;80:1–9.
196. Jin X, Muntean BS, Aal-Aaboda MS, et al. L-type calcium channel modulates cystic kidney phenotype. Biochim Biophys Acta 2014;1842:1518–1526.
197. Ramachandran KV, Hennessey JA, Barnett AS, et al. Calcium influx through L-type CaV1.2 Ca2+ channels regulates mandibular development. J Clin Invest 2013; 123:1638–1646.
198. Yu PC, Gu SY, Bu JW, et al. TRPC1 is essential for in vivo angiogenesis in zebrafish. Circ Res 2010;106: 1221–1232.
199. Inaba M, Yamanaka H, Kondo S. Pigment pattern formation by contact-dependent depolarization. Science 2012;335:677.
200. Iwashita M, Watanabe M, Ishii M, et al. Pigment pattern in jaguar/obelix zebrafish is caused by a Kir7.1 Mutation:

Implications for the regulation of melanosome movement. PLoS Genet 2006;2:e197.
201. Zhou H, Clapham DE. Mammalian MagT1 and TUSC3 are required for cellular magnesium uptake and vertebrate embryonic development. Proc Natl Acad Sci U S A 2009; 106:15750–15755.
202. Liao H, Chen Y, Li Y, et al. CFTR is required for the migration of primordial germ cells during zebrafish early embryogenesis. Reproduction 2018;156:261–268.
203. Irion U, Frohnhofer HG, Krauss J, et al. Gap junctions composed of connexins 41.8 and 39.4 are essential for colour pattern formation in zebrafish. Elife 2014;3: e05125.
204. Watanabe M, Iwashita M, Ishii M, et al. Spot pattern of leopard *Danio* is caused by mutation in the zebrafish connexin41.8 gene. EMBO Rep 2006;7:893–897.
205. Hoptak-Solga AD, Nielsen S, Jain I, et al. Connexin43 (GJA1) is required in the population of dividing cells during fin regeneration. Dev Biol 2008;317:541–548.
206. Iovine MK, Higgins EP, Hindes A, et al. Mutations in connexin43 (GJA1) perturb bone growth in zebrafish fins. Dev Biol 2005;278:208–219.
207. Sims K, Jr., Eble DM, Iovine MK. Connexin43 regulates joint location in zebrafish fins. Dev Biol 2009;327:410–418.
208. Robu ME, Larson JD, Nasevicius A, et al. p53 activation by knockdown technologies. PLoS Genet 2007;3:e78.
209. Hermle T, Guida MC, Beck S, et al. Drosophila ATP6AP2/VhaPRR functions both as a novel planar cell polarity core protein and a regulator of endosomal trafficking. EMBO J 2013;32:245–259.
210. Hermle T, Saltukoglu D, Grunewald J, et al. Regulation of Frizzled-dependent planar polarity signaling by a V-ATPase subunit. Curr Biol 2010;20:1269–1276.
211. Rujano MA, Cannata Serio M, Panasyuk G, et al. Mutations in the X-linked ATP6AP2 cause a glycosylation disorder with autophagic defects. J Exp Med 2017;214: 3707–3729.
212. Djiane A, Krejci A, Bernard F, et al. Dissecting the mechanisms of Notch induced hyperplasia. EMBO J 2013;32:60–71.
213. Doherty D, Jan LY, Jan YN. The Drosophila neurogenic gene big brain, which encodes a membrane-associated protein, acts cell autonomously and can act synergistically with Notch and Delta. Development 1997;124:3881–3893.
214. Hartenstein AY, Rugendorff A, Tepass U, et al. The function of the neurogenic genes during epithelial development in the Drosophila embryo. Development 1992; 116:1203–1220.
215. Rao Y, Bodmer R, Jan LY, et al. The big brain gene of Drosophila functions to control the number of neuronal precursors in the peripheral nervous system. Development 1992;116:31–40.
216. Charroux B, Royet J. Mutations in the Drosophila ortholog of the vertebrate Golgi pH regulator (GPHR) protein disturb endoplasmic reticulum and Golgi organization and affect systemic growth. Biol Open 2014;3:72–80.
217. Bauer R, Lehmann C, Fuss B, et al. The Drosophila gap junction channel gene innexin 2 controls foregut development in response to Wingless signalling. J Cell Sci 2002;115:1859–1867.
218. Bauer R, Lehmann C, Martini J, et al. Gap junction channel protein innexin 2 is essential for epithelial morphogenesis in the Drosophila embryo. Mol Biol Cell 2004; 15:2992–3004.
219. Lehmann C, Lechner H, Loer B, et al. Heteromerization of innexin gap junction proteins regulates epithelial tissue organization in Drosophila. Mol Biol Cell 2006;17:1676–1685.
220. Richard M, Hoch M. Drosophila eye size is determined by Innexin 2-dependent Decapentaplegic signalling. Dev Biol 2015;408:26–40.
221. Smendziuk CM, Messenberg A, Vogl AW, et al. Bidirectional gap junction-mediated soma-germline communication is essential for spermatogenesis. Development 2015;142:2598–2609.
222. Giuliani F, Giuliani G, Bauer R, et al. Innexin 3, a new gene required for dorsal closure in Drosophila embryo. PLoS One 2013;8:e69212.
223. Masly JP, Jones CD, Noor MA, et al. Gene transposition as a cause of hybrid sterility in Drosophila. Science 2006; 313:1448–1450.
224. Ocorr K, Reeves NL, Wessells RJ, et al. KCNQ potassium channel mutations cause cardiac arrhythmias in Drosophila that mimic the effects of aging. Proc Natl Acad Sci U S A 2007;104:3943–3948.
225. Humphrey JA, Hamming KS, Thacker CM, et al. A putative cation channel and its novel regulator: Cross-species conservation of effects on general anesthesia. Curr Biol 2007;17:624–629.
226. Simons M, Gault WJ, Gotthardt D, et al. Electrochemical cues regulate assembly of the Frizzled/Dishevelled complex at the plasma membrane during planar epithelial polarization. Nat Cell Biol 2009;11:286–294.
227. Paul SM, Ternet M, Salvaterra PM, et al. The Na+/K+ ATPase is required for septate junction function and epithelial tube-size control in the Drosophila tracheal system. Development 2003;130:4963–4974.
228. Schwabe T, Bainton RJ, Fetter RD, et al. GPCR signaling is required for blood-brain barrier formation in drosophila. Cell 2005;123:133–144.
229. Lipshitz HD, Kankel DR. Specificity of gene action during central nervous system development in *Drosophila melanogaster*: Analysis of the lethal (1) optic ganglion reduced locus. Dev Biol 1985;108:56–77.
230. Hattori Y, Usui T, Satoh D, et al. Sensory-neuron subtype-specific transcriptional programs controlling dendrite morphogenesis: Genome-wide analysis of Abrupt and Knot/Collier. Dev Cell 2013;27:530–544.
231. Pathak T, Agrawal T, Richhariya S, et al. Store-operated calcium entry through Orai is required for transcriptional maturation of the flight circuit in Drosophila. J Neurosci 2015;35:13784–13799.
232. Pathak T, Trivedi D, Hasan G. CRISPR-Cas-induced mutants identify a requirement for dSTIM in larval dopaminergic cells of *Drosophila melanogaster*. G3 (Bethesda) 2017;7:923–933.
233. Wegman LJ, Ainsley JA, Johnson WA. Developmental timing of a sensory-mediated larval surfacing behavior correlates with cessation of feeding and determination of final adult size. Dev Biol 2010;345:170–179.
234. Hevia CF, Lopez-Varea A, Esteban N, et al. A search for genes mediating the growth-promoting function of TGFbeta in the *Drosophila melanogaster* Wing Disc. Genetics 2017; 206:231–249.
235. Abraham DM, Wolf MJ. Disruption of sarcoendoplasmic reticulum calcium ATPase function in Drosophila leads to cardiac dysfunction. PLoS One 2013;8:e77785.

236. Periz G, Fortini ME. Ca(2+)-ATPase function is required for intracellular trafficking of the Notch receptor in Drosophila. EMBO J 1999;18:5983–5993.
237. Peabody NC, Diao F, Luan H, et al. Bursicon functions within the Drosophila CNS to modulate wing expansion behavior, hormone secretion, and cell death. J Neurosci 2008;28:14379–14391.
238. Luan H, Lemon WC, Peabody NC, et al. Functional dissection of a neuronal network required for cuticle tanning and wing expansion in Drosophila. J Neurosci 2006;26: 573–584.
239. Eid JP, Arias AM, Robertson H, et al. The Drosophila STIM1 orthologue, dSTIM, has roles in cell fate specification and tissue patterning. BMC Dev Biol 2008;8:104.
240. Georgiev P, Okkenhaug H, Drews A, et al. TRPM channels mediate zinc homeostasis and cellular growth during Drosophila larval development. Cell Metab 2010;12:386–397.
241. Hofmann T, Chubanov V, Chen X, et al. Drosophila TRPM channel is essential for the control of extracellular magnesium levels. PLoS One 2010;5:e10519.
242. Sandstrom DJ. Extracellular protons reduce quantal content and prolong synaptic currents at the Drosophila larval neuromuscular junction. J Neurogenet 2011;25:104–114.
243. Wong CO, Palmieri M, Li J, et al. Diminished MTORC1-dependent JNK activation underlies the neurodevelopmental defects associated with lysosomal dysfunction. Cell Rep 2015;12:2009–2020.
244. Smith HK, Luo L, O'Halloran D, et al. Defining specificity determinants of cGMP mediated gustatory sensory transduction in *Caenorhabditis elegans*. Genetics 2013; 194:885–901.
245. Avery L. The genetics of feeding in *Caenorhabditis elegans*. Genetics 1993;133:897–917.
246. Shephard F, Adenle AA, Jacobson LA, et al. Identification and functional clustering of genes regulating muscle protein degradation from amongst the known *C. elegans* muscle mutants. PLoS One 2011;6:e24686.
247. Watson E, MacNeil LT, Arda HE, et al. Integration of metabolic and gene regulatory networks modulates the *C. elegans* dietary response. Cell 2013;153:253–266.
248. Troemel ER, Sagasti A, Bargmann CI. Lateral signaling mediated by axon contact and calcium entry regulates asymmetric odorant receptor expression in *C. elegans*. Cell 1999;99:387–398.
249. Kamath RS, Fraser AG, Dong Y, et al. Systematic functional analysis of the *Caenorhabditis elegans* genome using RNAi. Nature 2003;421:231–237.
250. Trent C, Tsuing N, Horvitz HR. Egg-laying defective mutants of the nematode *Caenorhabditis elegans*. Genetics 1983;104:619–647.
251. Kwok TC, Hui K, Kostelecki W, et al. A genetic screen for dihydropyridine (DHP)-resistant worms reveals new residues required for DHP-blockage of mammalian calcium channels. PLoS Genet 2008;4:e1000067.
252. Berry KL, Bulow HE, Hall DH, et al. A *C. elegans* CLIC-like protein required for intracellular tube formation and maintenance. Science 2003;302:2134–2137.
253. Davis MW, Fleischhauer R, Dent JA, et al. A mutation in the *C. elegans* EXP-2 potassium channel that alters feeding behavior. Science 1999;286:2501–2504.
254. Hu J, Barr MM. ATP-2 interacts with the PLAT domain of LOV-1 and is involved in *Caenorhabditis elegans* polycystin signaling. Mol Biol Cell 2005;16:458–469.
255. Ghosh S, Sternberg PW. Spatial and molecular cues for cell outgrowth during *C. elegans* uterine development. Dev Biol 2014;396:121–135.
256. Sarin S, O'Meara MM, Flowers EB, et al. Genetic screens for *Caenorhabditis elegans* mutants defective in left/right asymmetric neuronal fate specification. Genetics 2007; 176:2109–2130.
257. Komatsu H, Mori I, Rhee JS, et al. Mutations in a cyclic nucleotide-gated channel lead to abnormal thermosensation and chemosensation in *C. elegans*. Neuron 1996;17: 707–718.
258. Chen CH, Lee A, Liao CP, et al. RHGF-1/PDZ-RhoGEF and retrograde DLK-1 signaling drive neuronal remodeling on microtubule disassembly. Proc Natl Acad Sci U S A 2014;111:16568–16573.
259. Tavernarakis N, Shreffler W, Wang S, et al. unc-8, a DEG/ENaC family member, encodes a subunit of a candidate mechanically gated channel that modulates *C. elegans* locomotion. Neuron 1997;18:107–119.
260. Zhu H, Duerr JS, Varoqui H, et al. Analysis of point mutants in the *Caenorhabditis elegans* vesicular acetylcholine transporter reveals domains involved in substrate translocation. J Biol Chem 2001;276:41580–41587.
261. Green RA, Kao HL, Audhya A, et al. A high-resolution *C. elegans* essential gene network based on phenotypic profiling of a complex tissue. Cell 2011;145:470–482.
262. Chuang CF, Vanhoven MK, Fetter RD, et al. An innexin-dependent cell network establishes left-right neuronal asymmetry in *C. elegans*. Cell 2007;129:787–799.
263. Bellemer A, Hirata T, Romero MF, et al. Two types of chloride transporters are required for GABA(A) receptor-mediated inhibition in *C. elegans*. EMBO J 2011;30: 1852–1863.
264. Chen S, Spence AM, Schachter H. Isolation of null alleles of the *Caenorhabditis elegans* gly-12, gly-13 and gly-14 genes, all of which encode UDP-GlcNAc: Alpha-3-D-mannoside beta1,2-N-acetylglucosaminyltransferase I activity. Biochimie 2003;85:391–401.
265. Park EC, Horvitz HR. Mutations with dominant effects on the behavior and morphology of the nematode *Caenorhabditis elegans*. Genetics 1986;113:821–852.
266. Axang C, Rauthan M, Hall DH, et al. Developmental genetics of the *C. elegans* pharyngeal neurons NSML and NSMR. BMC Dev Biol 2008;8:38.
267. Yeh E, Ng S, Zhang M, et al. A putative cation channel, NCA-1, and a novel protein, UNC-80, transmit neuronal activity in *C. elegans*. PLoS Biol 2008;6:e55.
268. Sedensky MM, Meneely PM. Genetic analysis of halothane sensitivity in *Caenorhabditis elegans*. Science 1987; 236:952–954.
269. Schmitz C, Kinge P, Hutter H. Axon guidance genes identified in a large-scale RNAi screen using the RNAi-hypersensitive *Caenorhabditis elegans* strain nre-1(hd20) lin-15b(hd126). Proc Natl Acad Sci U S A 2007;104:834–839.
270. Takayama K, Muto A, Kikuchi Y. Leucine/glutamine and v-ATPase/lysosomal acidification via mTORC1 activation are required for position-dependent regeneration. Sci Rep 2018;8:8278.
271. Monteiro J, Aires R, Becker JD, et al. V-ATPase proton pumping activity is required for adult zebrafish appendage regeneration. PLoS One 2014;9:e92594.

272. Finbow ME, Pitts JD. Structure of the ductin channel. Biosci Rep 1998;18:287–297.
273. Pietrantonio PV, Gill SS. Ductin, a component of the V-ATPase, is developmentally regulated in Heliothis virescens midgut, and anti-ductin antibodies label lateral membranes. Cell Tissue Res 1997;289:97–108.
274. Banerji R, Eble DM, Iovine MK, et al. Esco2 regulates cx43 expression during skeletal regeneration in the zebrafish fin. Dev Dyn 2016;245:7–21.
275. Meier C, Rosenkranz K. Cx43 expression and function in the nervous system-implications for stem cell mediated regeneration. Front Physiol 2014;5:106.
276. Oviedo NJ, Morokuma J, Walentek P, et al. Long-range neural and gap junction protein-mediated cues control polarity during planarian regeneration. Dev Biol 2010; 339:188–199.
277. Oviedo NJ, Levin M. smedinx-11 is a planarian stem cell gap junction gene required for regeneration and homeostasis. Development 2007;134:3121–3131.

Address correspondence to:
Michael Levin, PhD
Department of Biology
Allen Discovery Center
Tufts University
200 Boston Avenue
Suite 4600
Medford, MA 02155-4243
USA

E-mail: michael.levin@tufts.edu